Enhanced antimalarial activity of plasmepsin V inhibitors by modification of the P_2 position of PEXEL peptidomimetics

William Nguyen,[†,‡] Anthony N. Hodder,[†,‡] Richard Bestel de Lezongard,[†,‡] Peter E. Czabotar, [†,‡] Kate E. Jarman,[†,‡] Matthew T. O'Neill,[†] Jennifer K. Thompson,[†] Helene Jousset Sabroux,[†,‡] Alan F. Cowman,[†,‡] Justin A. Boddey[†,‡] and Brad E. Sleebs.[,†,‡]*

[†] The Walter and Eliza Hall Institute of Medical Research, Parkville, 3052, Australia.

[‡] Department of Medical Biology, The University of Melbourne, Parkville, 3010, Australia.

* Corresponding Author: Brad E. Sleebs, The Walter and Eliza Hall Institute of Medical Research, 1G Royal Parade, Parkville 3052, Victoria, Australia. Phone: +61 3 9345 2718; Email: sleebs@wehi.edu.au

KEYWORDS: plasmepsin, Malaria, protease, peptidomimetic, PEXEL, trafficking.

ABSTRACT

Plasmepsin V is an aspartyl protease that plays a critical role in the export of proteins bearing the *Plasmodium* export element (PEXEL) motif (RxLxQ/E/D) to the infected host erythrocyte, and thus the survival of the malaria parasite. Previously, development of transition state PEXEL mimetic inhibitors of plasmepsin V have primarily focused on demonstrating the importance of the P_3 Arg and P_1 Leu in binding affinity and selectivity. Here, we investigate the importance of the P_2 position by incorporating both natural and non-natural amino acids into this position and show disubstituted beta-carbon amino acids convey the greatest potency. Consequently, we show analogues with either cyclohexylglycine or phenylglycine in the P_2 position are the most potent inhibitors of plasmepsin V that impair processing of the PEXEL motif in exported proteins resulting in death of *P. falciparum* asexual stage parasites.

INTRODUCTION

The World Health Organization estimates that around 3.5 billion people, about half of the world's population, live at risk of malaria [1]. Malaria is caused by *Plasmodium* parasites and results in approximately 460,000 deaths annually [1]. *P. falciparum* and *P. vivax* are the most virulent species, accounting for 75% and 20% of cases worldwide, respectively. There is currently a strong commitment to eliminate malaria in the 21st century. However, the current arsenal of clinically used artemisinin combination therapies and drug candidates undergoing clinical assessment may not be sufficient to eliminate the disease, due to the threat of emerging drug resistance [2, 3]. Thus, new agents are required that target multiple stages of the malaria parasite's lifecycle with novel mechanisms of action.

Genome sequencing uncovered the *P. falciparum* parasite expresses ten cathepsin D-like or A1 family aspartyl proteases, known as plasmepsins (PMs). The PMs have diverse roles across the parasite's lifecycle and several essential PMs are considered attractive antimalarial drug targets. PMs I, II, IV and histo-aspartyl protease (HAP) are localised to the digestive vacuole of the asexual parasite and degrade hemoglobin providing sustenance for the parasite [4, 5], but genetic studies have established these PMs are not essential for parasite survival [5-9] and thus not viable antimalarial targets. PMs VI-VIII are not expressed in the asexual stage of the parasite, but PMVI and PMVIII have undefined but essential roles in *P. berghei* within the mosquito stage [10, 11], while PMVII is not essential in *P. berghei* [12]. The role of PMs VI, VII and VIII in species that infect humans is not known and thus additional evidence is required to confirm their validity as drug targets. PMIX has an indispensable role in invasion and PMX is essential for both invasion and egress of the erythrocyte and both are considered potential antimalarial drug targets [13, 14].

Several PMs have been targeted with small molecules with varying degrees of success[13-22], but none have progressed to the clinic.

An important feature of malaria parasite survival is the remodeling of the host erythrocyte environment. A key event that underpins the remodeling process is the transport of many hundreds of parasite proteins into the erythrocyte [23-25]. Exported proteins play critical roles in parasite survival, such as providing sustenance for the parasite to replicate, evasion of the host immune system and nutrient and waste efflux from the host erythrocyte [26]. Approximately 460 proteins destined for export possess an N-terminal motif with the consensus sequence RxLxQ/E/D, known as the *Plasmodium* export element (PEXEL) [27], or vacuolar targeting sequences (VTS) [28]. For proteins to be exported, the endoplasmic reticulum resident aspartyl protease, PMV processes the PEXEL motif at the C-terminal amide bond of leucine [29, 30]. The processing event is an essential step in the export of PEXEL containing-proteins [23, 29-32] and for export of PEXEL-negative proteins because the latter require PEXEL proteins for their trafficking for the survival of the malaria parasite in erythrocyte [23, 26, 33]. PMV and PEXEL proteins are highly conserved in all *Plasmodium* species including the most virulent species, *P. falciparum* [25].

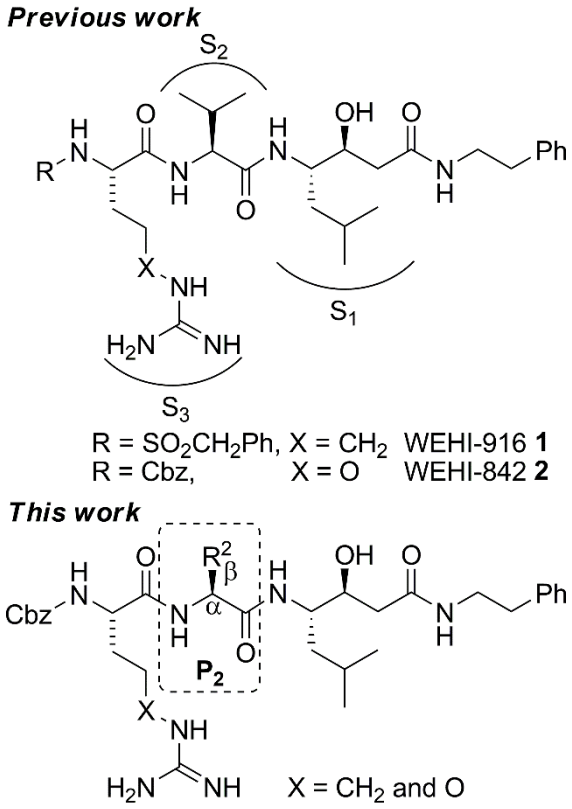

Figure 1. The structures of WEHI-916 **1** and WEHI-842 **2** shown occupying substrate binding pockets of PMV, and the relationship to the work undertaken here focusing on the P_2 region.

Recently, it was shown transition state peptidomimetics that mimic the native PEXEL motif, RxL, are potent inhibitors of both *P. vivax* and *P. falciparum* PMV. The earliest example, WEHI-916 **1** (Fig 1) [34, 35], was shown to prevent processing and export of PEXEL containing proteins resulting in death of *P. falciparum* asexual stage parasites *in vitro*. A subsequent study established that replacing the P_3 Arg in **1** with canavanine (Cav) produced the analogue named WEHI-842 **2** [36, 37], (Fig 1) which possessed a 10-fold improvement in affinity for PMV and for killing *P. falciparum* compared to **1**. An X-ray structure of **2** bound to PMV was also obtained and illustrated key binding interactions that described the requirement of the RxL motif for binding to PMV [37].

These studies further corroborated biological evidence that PMV plays a vital role in protein export and that this process is essential for parasite survival, thus reinforcing PMV as a promising antimalarial target.

The critical nature of the P_3 Arg and P_1 Leu in the PEXEL motif has been well studied [23, 29, 30, 34-36, 38, 39] (Fig 5), but the importance of the P_2 region remains largely unknown. The limited studies describing the P_2 region show that both Val (seen in **1** and **2**, Fig 1) and Ile appear optimal, while analogues that possess a P_2 Ala, Phe or Leu have lower affinity for PMV [34]. This and unpublished data from our laboratory led to the hypothesis that peptidomimetics that harbor a P_2 amino acid with di-substitution at the beta-carbon (Fig 1) have greater affinity for PMV than those analogues without this substitution pattern.

Herein, we explore the P_2 region by way of substituting both natural and non-natural amino acids into the RxL mimetic scaffold. The amino acids selected for integration of the P_2 position would test our hypothesis that beta di-substitution is important for improving PMV potency. Thus, amino acids such as cyclopentylglycine, phenylglycine were selected, but also amino acids that did not possess beta di-substitution to serve as controls, such as phenylalanine and norvaline. There were several other factors that influenced our choice of amino acid for the P_2 motif. The first was the selection of amino acids that possessed hydrophobic side chains because the S_2 binding cavity is mostly lined with hydrophobic amino acids, as shown in the X-ray structure of **2** bound to PMV (Fig 2). Hydrophobic amino acids were also chosen to increase overall lipophilicity of peptidomimetic analogues to assist in membrane permeability. Lastly, there was an emphasis on selecting non-natural and non-essential amino acids, as it was reasoned that these amino acids may impart greater metabolic stability, given they would not be readily recognized by other proteases compared to the 20 proteinogenic amino acids.

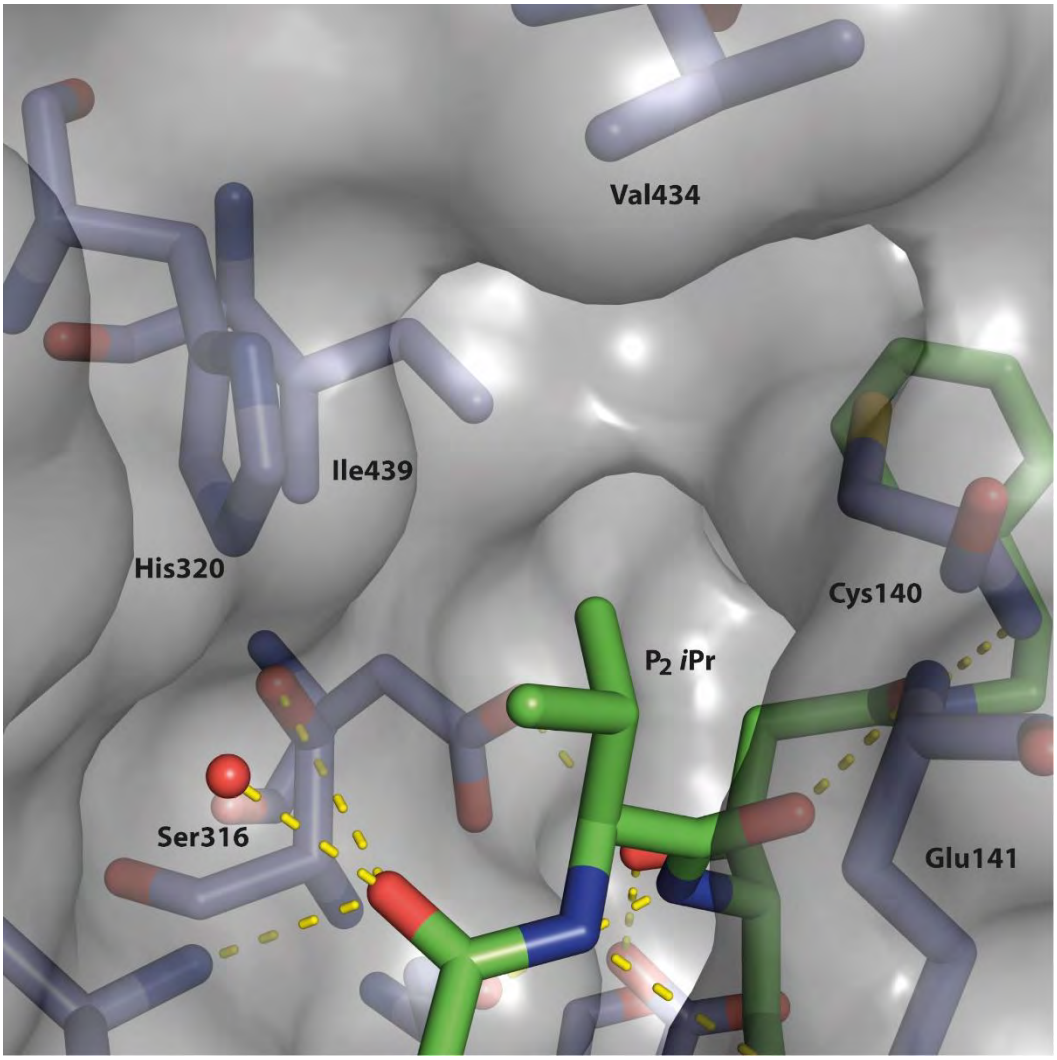

Figure 2. The S_2 substrate binding cavity of PMV (grey surface and blue amino acids) occupied by the P_2 *i*Pr group of WEHI-842 **2** (green). The image was created using the X-ray structure of **2** bound to *P. vivax* PMV (PDB: 4ZL4).[37] Hydrogen bonds between **2** and PMV are highlighted with yellow-dotted lines.

Previous studies have shown the incorporation of Cav into the P_3 position of PEXEL mimetics are 10-fold more potent than the Arg orthologue (see **1** versus **2** in Table 1 for comparison) [36, 37]. However, due to the ease of access and availability of Arg compared with Cav, we first

incorporated Arg into all P_2 analogues. We then proposed to integrate Cav into the P_3 position of the analogues that possess the greatest affinity for PMV. In earlier studies [34, 36], the N-terminal Cbz and C-terminal $NH(CH_2)_2Ph$ functionalities, seen in **2** (Fig 1 and 5), were shown to be optimal, and thus would remain the same for the analogues produced in the present study.

RESULTS AND DISCUSSION

Chemistry

Exploration of the P_2 site begun with the synthesis of analogues. We used solution phase peptide synthesis following established procedures in literature [34, 36, 39] to construct analogues (Scheme 1). Briefly, the synthesis started with coupling the commercially available Boc-protected amino acid **3** with the NH_2-Sta(*S,S*)-$NH(CH_2)_2Ph$ to produce dipeptide **4**. We found that directly accessing the tripeptide **6** by coupling Cbz-Arg(*N,N*-diBoc)-OH to the Boc de-protected dipeptide **4**, was low yielding. To circumvent this issue, the dipeptide **4** were Boc deprotected and coupled to Cbz-Orn(*N*-Boc)-OH to give the tripeptide **5**. The Orn(*N*-Boc) functionality on **5** was then transformed to Arg(*N,N*-diBoc) over two steps to yield the tripeptide **6**. At this stage, Cbz-Cav(*N*-Boc)-OH was also introduced, by coupling to the Boc deprotected dipeptide **4** to produce the Cav analogue **7**. Finally, the Boc groups were removed from **6** and **7**. However, in this deprotection we discovered a trifluoroacetamide byproduct. The trifluoroacetamide byproduct has been reported with similar chemistries in the past [40, 41], but it was unknown mechanistically why this byproduct was observed in this instance. To overcome this issue, we removed the trifluoroacetamide group using K_2CO_3 in MeOH, then TFA was applied to give the TFA salts of the tripeptide products **8-28**.

Scheme 1. General synthetic pathway to access P_2 analogues.

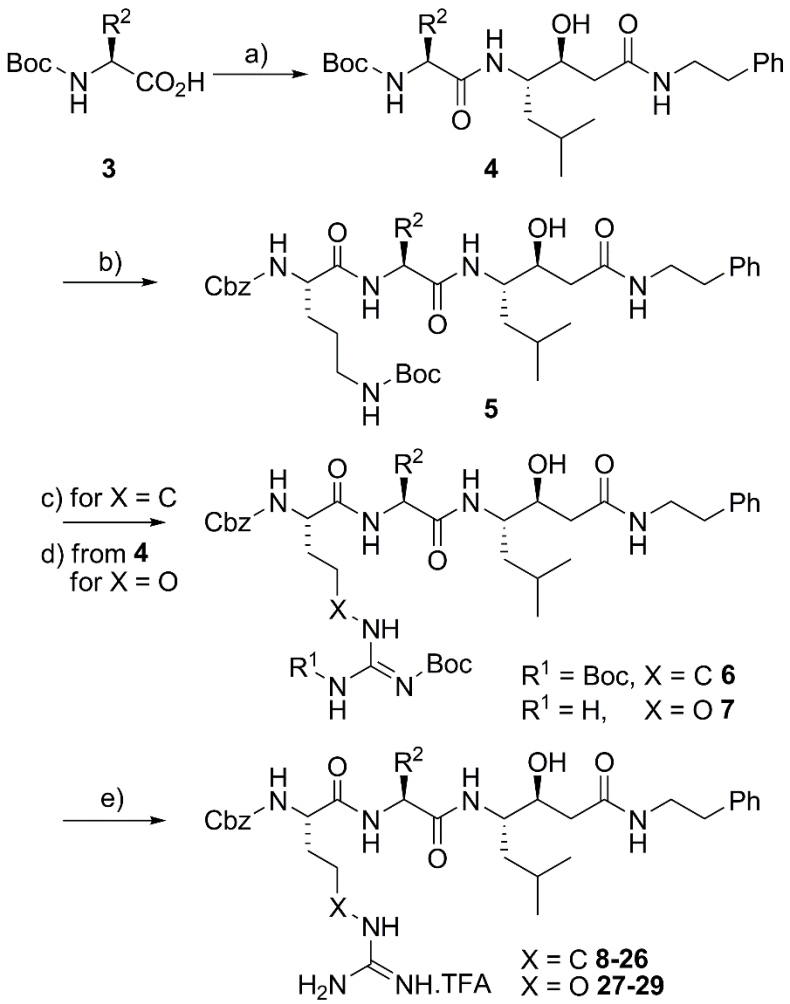

Reagents and conditions: a) HCl.NH_2-Sta(S,S)-$NH(CH_2)_2$Ph (from ref [34, 35]), HBTU, DIPEA, DMF; b) i) 4N HCl; ii) Cbz-Orn(N-Boc)-OH, HBTU, DIPEA, DMF; c) i) 4N HCl; ii) N,N'-bis-Boc-1-guanylpyrazole, DIPEA, DCM; d) i) 4N HCl; ii) Cbz-Cav(N-Boc)-OH (from ref [36, 37]), DIPEA, HBTU, DMF; e) i) TFA, DCM; ii) K_2CO_3, MeOH; iii) TFA. For R^2 refer to Table 1.

Structure and activity relationship

To assess the effect that the P_2 modifications have on PMV activity, compounds **8-28** were evaluated using the previously described fluorogenic assay format [36]. Briefly, compounds were assessed for their ability to block cleavage of a fluorogenic peptide containing the RTLAQ PEXEL

sequence of the exported protein KAHRP (Knob-associated histidine-rich protein) [42] by recombinant *P. vivax* PMV [37]. We have included benchmark compounds **1** and **2** for comparison of assay performance in this study compared to that in previous studies [34-36, 39]. Of note, analogue **11** that possesses an *i*Pr in the P_2 position has similar activity to the previously described **1** [34, 35] in this assay format. The results of the PMV assay are summarized in Table 1.

The results of the PMV assay show that small aliphatic substituents in the P_2 position, such as Me, Et and *n*Pr (**9-11**), have increasing modest affinity for PMV (IC_{50} 7.2, 0.51, and 0.12 μM respectively). Compounds with larger aliphatic substituents, such as *i*Pr, *i*Bu, *s*Bu and $CH(Et)_2$ (**11-13** and **15**) have improved potencies (IC_{50} 0.12, 0.17, 0.03 and 0.11 μM respectively) compared with the smaller substituents. Notably, analogues that harbor beta-disubstitution, such as *i*Pr, *s*Bu and $CH(Et)_2$ (**11**, **13** and **15**) are more active than *n*Pr and *i*Bu (**11** and **12**) arguably supporting the hypothesis that beta-disubstitution is important for PMV potency. Further supporting this notion, *s*Bu, CyPen, CyHex and Ph (**13**, **16-18**) in the P_2 position were found to be the most potent analogues in this study (IC_{50} 0.026, 0.055, 0.024 and 0.029 μM respectively). Analogue **14** with a *t*Bu at the P_2 position, was not well tolerated (IC_{50} 6.7 μM). It is possible that the extra steric bulk at the beta-carbon was not accommodated by the S_2 binding pocket of PMV.

Table 1. Biological activities and calculated properties of analogues.

Cmpd No.	X [a]	R^2 [a]	PMV IC_{50} (SD) (μM) [b]	Pf parasite EC_{50} (SD) (μM) [c]	HepG2 EC_{50} (SD) (μM) [d]	cLogP [e]	LipE [f]
8	CH_2	Me	7.18 (3.06)	>10.0	>40	1.4	3.65
9	CH_2	Et	0.507 (0.14)	3.14 (0.83)	>40	1.9	4.32
10	CH_2	*n*Pr	0.116 (0.26)	2.40 (0.54)	n.d.	2.4	4.55
11	CH_2	*i*Pr	0.116 (0.033)	3.39 (1.14)	>40	2.3	4.36
12	CH_2	*i*Bu	0.165 (0.005)	5.00 (2.27)	>40	2.7	4.11
13	CH_2	*S*-sBu	0.026 (0.002)	1.03 (0.16)	n.d.	2.8	4.83
14	CH_2	*t*Bu	6.70 (0.490)	>10.0	>40	2.7	2.48
15	CH_2	$CH(Et)_2$	0.112 (0.013)	4.11 (0.66)	>40	3.2	3.74
16	CH_2	CyPen	0.055 (0.015)	2.73 (0.59)	>40	2.7	4.52
17	CH_2	CyHex	0.029 (0.011)	1.22 (0.28)	36.7 (0.4)	3.2	4.36
18	CH_2	Ph	0.024 (0.005)	1.36 (0.74)	>40	2.7	4.88
19	CH_2	Bzl	3.12 (0.470)	>10.0	>40	3.1	2.24
20	CH_2	$CH(Ph)_2$	>10.0	>10.0	>40	4.6	-
21	CH_2	CH(Me)Ph [g]	>10.0	>10.0	35.4 (1.5)	3.4	-
22	CH_2	2-indane	0.661 (0.370)	6.18 (1.64)	23.5 (1.0)	3.5	2.82
23	CH_2	CH_2OH	>10.0	>10.0	>40	0.3	-
24	CH_2	$C(OH)(Me)_2$	3.01 (0.90)	>10.0	>40	1.0	4.49
25	CH_2	*R*-CH(OH)Me	2.02 (0.28)	>10.0	>40	0.7	4.95
26	CH_2	CH(OH)Ph [h]	6.56 (1.09)	>10.0	>40	2.1	3.08
27	O	CyHex	0.005 (0.001)	0.09 (0.07)	>40	3.1	5.15
28	O	Ph	0.003 (0.001)	0.07 (0.01)	>40	2.8	5.79
29	O	*S*-sBu	0.016 (0.003)	0.18 (0.054)	n.d.	2.7	5.09
1 [i]	CH_2	*i*Pr	0.123 (0.020)	4.03 (0.83)	>40	1.3	5.59
2	O	*i*Pr	0.019 (0.007)	0.43 (0.14)	>40	2.3	5.45

[a] Refer to Figure 1. [b] IC_{50} data represents means and SD for three independent fluorogenic substrate cleavage experiments. A 10-point dilution series of each compound was incubated (37 °C) with recombinant *P. vivax* PMV. [c] EC_{50} data represents means and SD for three independent experiments measuring LDH activity of *P. falciparum* 3D7 parasites following exposure to compounds in 10-point dilution series for 72 h. Chloroquine EC_{50} 0.006 μM; mefloquine EC_{50}

0.013 μM. [d] EC_{50} data represents means and SD for three HepG2 cell growth inhibition experiments. A 10-point dilution series of each compound incubated (37 ºC) for 48 h. Cell Titer-Glo was used to quantify cell viability. Bortezomib EC_{50} 0.01 μM; chloroquine EC_{50} 10.1 μM; mefloquine EC_{50} 9.8 μM. [e] Calculated using ChemAxon software.[43] [f] Calculated using PMV IC_{50} values. [g] L-*erythro* configured. [h] D,L-*threo* configured. [i] refer to Fig 1 for structure of **1**. n.d. – no data.

Analogue **19**, supporting a benzyl group in the P_2 position, displayed modest activity against PMV (IC_{50} 3.1 μM) compared to analogues **9-13** and **15-17** with aliphatic P_2 groups (all with IC_{50}s <0.6 μM). In this instance, disubstitution at the beta-carbon of benzyl-like analogues **20**, **21** and **26**, did not improve potency (IC_{50} >10, >10 and 6.6 μM respectively) compared to the benzyl analogue **19** (IC_{50} 3.1 μM). It is noted that the stereochemistry of the beta-methyl (L-*erythro* configured) and hydroxy (D,L-*threo* configured) may have impacted the PMV activity of compounds **21** and **26**, respectively. The exception was **22**, which possesses a 2-indane at the P_2 site, that was more potent than the benzyl analogue **19** (IC_{50} 0.66 versus 3.1 μM). The difference in activity between the beta methyl benzyl (**21**) and the 2-indane (**22**) is likely due to restricted rotation of the phenyl ring of the 2-indane moiety that conferred a more favorable orientation for binding to the S_2 pocket of PMV.

Compounds **23-26** that possess a hydroxyl at the beta-carbon of the P_2 position displayed weak activity against PMV (all with IC_{50}s >2 μM). For example, analogues **23** and **24** that possess CH_2OH (Ser) and CH(OH)Me (Thr) in the P_2 position, (IC_{50} >10 and 3 μM) compared to analogues **9** and **11**, that have Et and *i*Pr aliphatic groups of similar steric bulk (IC_{50} 0.55 and 0.11 μM). It was reasoned that the modest PMV activity of the beta-hydroxy analogues **23-26** is due to the relatively hydrophobic nature of amino acids that line the S_2 pocket of PMV (Fig 2).

By examining which functionalities in the P_2 position imparted the greatest potency against PMV, we identified that *s*Bu, CyHex and Ph (**13**, **17** and **18**) were most optimal. We next studied the effect of replacing the Arg in the P_3 position of **13**, **17** and **18** with Cav. Previous studies have shown that **2**, which possesses a P_3 Cav, is 10-fold more potent than **1** that has a P_3 Arg (Fig 1) [36, 37]. Our data here confirms this observation, with IC_{50} values of 0.119 and 0.019 μM for **1** and **2** respectively (Table 1). Two analogues, **27-28** with Cav at the P_3 position and CyHex, and Ph at the P_2 sites were generated and showed a 6 to 8-fold improvement in PMV potency (IC_{50} 0.005 and 0.003 μM) compared with the P_3 Arg comparator analogues **17** and **18** (IC_{50} 0.029 and 0.024 μM). This supports the previous observations that Cav significantly enhances PMV inhibitory activity compared with analogues possessing Arg at the P_3 position. The potency difference between the *s*Bu analogues **13** and **29** was only 2-fold and was not as significant as observed with other Cav and Arg analogues, such as **1** and **2**. Compound **13** was the most potent P_3 Arg analogue, but the fold improvement in potency between **13** and the P_3 Cav analogue **29** was not as significant as the fold change between other P_3 Arg and P_3 Cav orthologues, for example the 10-fold improvement between **1** and **2**. As a result, we concentrated on using the S_2 CyHex and Ph analogues, **17**, **18**, **27** and **28** in further biological and structural analyses.

To examine whether lipophilicity was a contributing factor in the increase of analogue potency, lipophilic efficiency (LipE) was calculated (Table 1). From these calculations, it is observed that even though cLogP generally increases with PMV potency, the LipE values also increase, indicating the improvement in potency observed (for example, from analogue **8** (Me) to **18** (Ph) with respective LipE values of 3.65 and 4.88), is not solely due to the overall increase in hydrophobicity.

Structural Basis of PMV inhibition

To understand the structural basis for the inhibition of PMV by the analogues, we obtained an X-ray crystal structure of **27** (WEHI-601) bound to PMV (PDB: 6C4G). The structure obtained at a resolution of 2.6Å was almost identical to the previous X-ray structure (4ZL4) of **2** bound to PMV [37]. One notable difference between the structures was the presence of N-glycosylated Asn280 and Asn355 (Fig S1 and S2), a result of using SF21 insect cells to express the protein. N-glycosylation of Asn355 was thought to have occurred in 4ZL4, but poorly defined density in this region of the crystal structure prevented building in the N-glycosylation with confidence [37]. Another difference was the perturbation of the helix-turn-helix motif, compared to 4ZL4 (Fig S1). The X-ray structure also showed that **27** bound to the substrate binding cleft of PMV in a similar conformation and possessing the same hydrogen bond interactions found with **2** in 4ZL4 (Fig S3). Compared to the P_2 *i*Pr group of **2**, the P_2 CyHex of **27** almost completely occupied the S_2 pocket of PMV (Fig 3). This occupancy may explain the increase in potency of **27** compared with **2** (Fig 2 and Table 1).

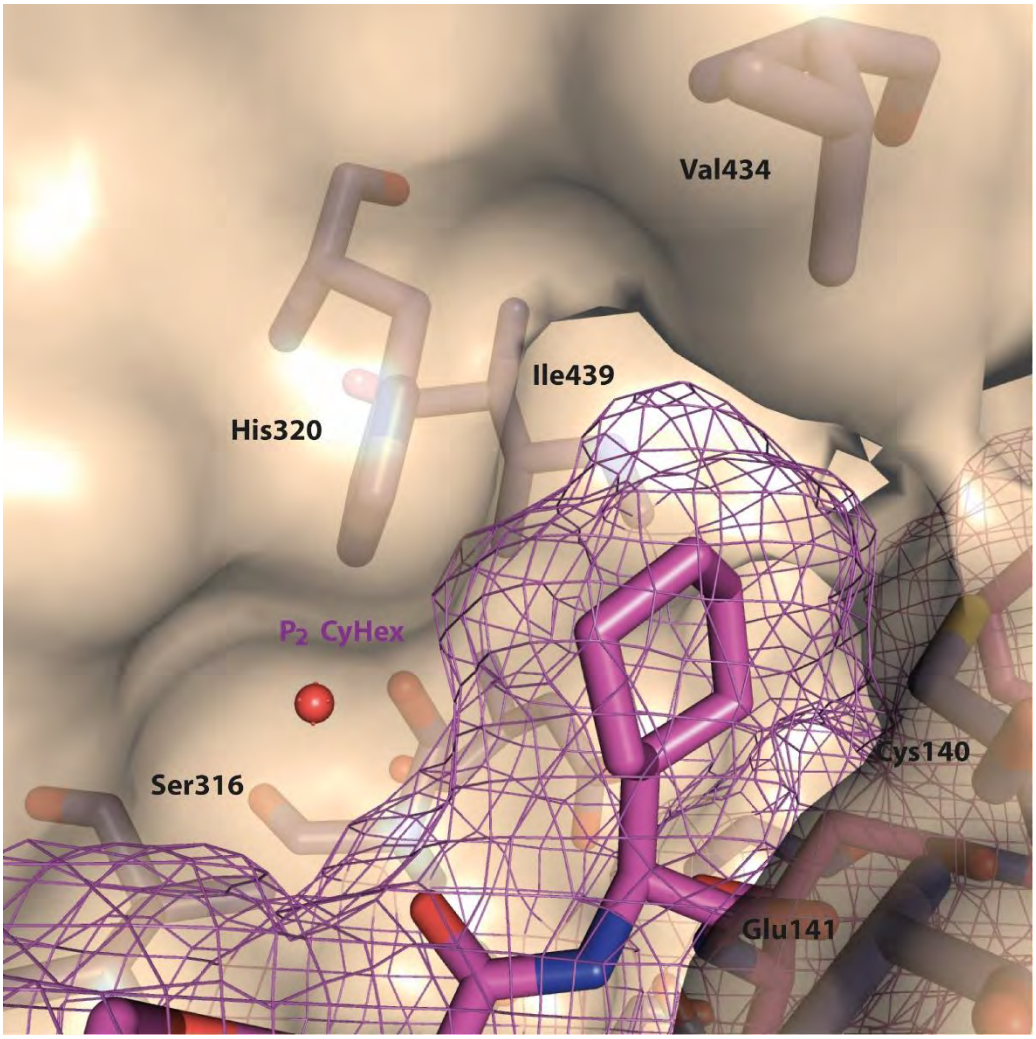

Figure 3. The X-ray structure of *P. vivax* PMV bound to **27** (WEHI-601) (PDB: 6C4G). Shown is the S_2 substrate binding cavity of PMV (orange surface and blue amino acids) occupied by the P_2 CyHex group of **27** (stick and mesh in magenta).

To further explore the relationship between the structure and PMV activity of analogues we performed docking studies. In the docking studies, the X-ray crystal structure of **2** bound to PMV[37] was used as a template to dock analogues **8-26**. The results are shown in Fig S4-7. In general, the docking studies support the PMV assay data, in that the hydrophobic S_2 pocket is optimally occupied by either a P_2 CyHex and Ph (**17** and **18**). The docking of P_2 CyHex **17** was

supported by the X-ray structure of the CyHex of **27** occupying the S_2 pocket of PMV. It was found that smaller P_2 substituents, such Me, Et, Pr, *i*Pr, don't fully occupy the S_2 cavity and are accordingly less active than **17** and **18**. The modest activity of **19**, can be attributed to the steric size of its P_2 benzyl substituent that cannot be accommodated by the S_2 pocket, and thus is forced to orientate into solvent space. Docking also provides a possible explanation for why beta-disubstitution is important for PMV binding affinity. Firstly, the substitution pattern appears to restrict rotation of substitution at the beta-carbon that is optimal for binding, and secondly, provides the steric capacity to fully occupy the S_2 of PMV, thus providing a possible explanation why analogues without the beta-disubstitution pattern are generally less active.

Activity of analogues in *P. falciparum* parasites and human cells *in vitro*

To establish whether analogues **17**, **18**, **27** and **28** directly inhibit PMV in *P. falciparum* parasites *in vitro*, we assessed their ability to impair the processing of the exported protein *P. falciparum* erythrocyte membrane protein 3 fused to green fluorescent protein (PfEMP3-GFP). Using previously described protocols [29, 35], we treated the *P. falciparum* parasite line expressing PfEMP3-GFP with compounds **17**, **27** (Fig S10), **18**, and **28** (Fig 4), and used an anti-GFP antibody to determine the processing pattern of PfEMP3-GFP by western blot. This showed that the P_3 Cav analogues **27** and **28** cause accumulation of uncleaved PfEMP3-GFP to a greater extent than the P_3 Arg orthologues **17** and **18**. Furthermore, **27** and blocked PfEMP3-GFP processing more than **2**, consistent with these compounds inhibiting recombinant PMV more potently than **2** (Table 1). Thus, the trends in potency seen against recombinant PMV correlate well with the degree of PEXEL cleavage inhibition observed in the *P. falciparum*-infected erythrocyte PfEMP3 processing assay.

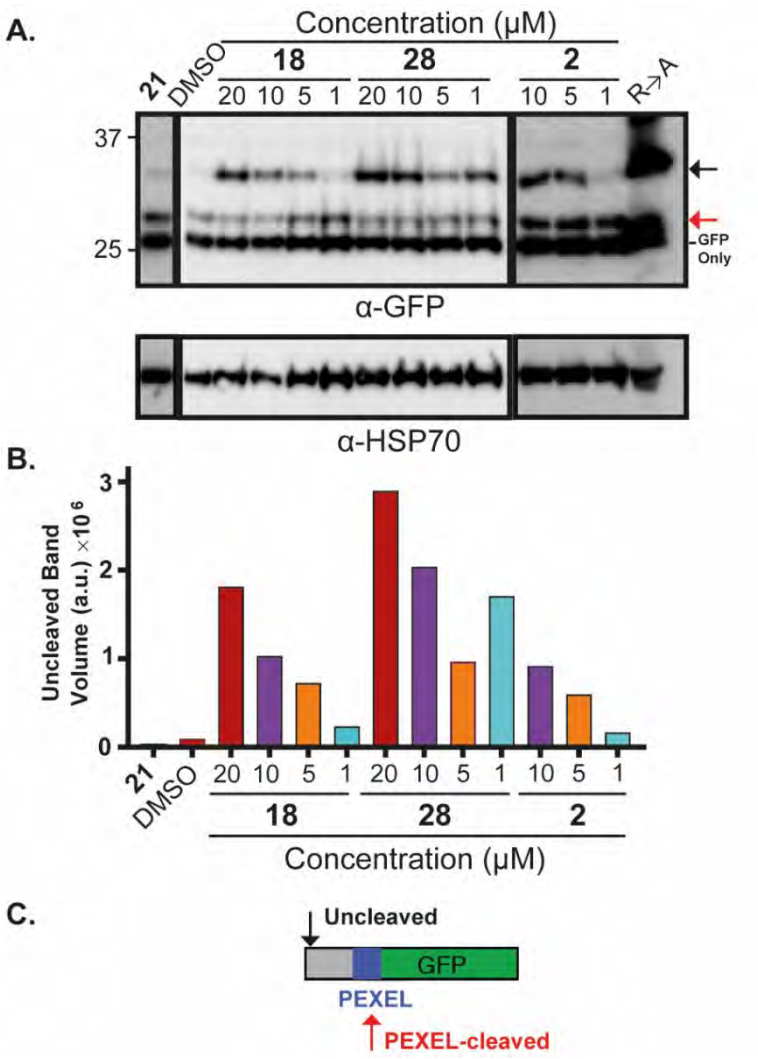

Figure 4. Inhibition of PEXEL processing by selected P_2 analogues in erythrocytes infected with *P. falciparum* 3D7 expressing PfEMP3-GFP. A) Infected erythrocytes were treated with compounds **18**, **28** and **2**[37] at the indicated concentration, **21** (20 μM) or vehicle control (DMSO). Processing of the PEXEL in PfEMP3 was assessed by immunoblotting with anti-GFP antibodies. Uncleaved (black arrow), PEXEL-cleaved (red arrow), and 'GFP only' (a degraded remnant of the GFP reporter in the food vacuole) species of PfEMP3-GFP are indicated next to the immunoblot and schematically represented in panel C. PEXEL R to A mutant PfEMP3-GFP was included as a size control, and the blot was probed with parasite anti-HSP70 as a loading control. B) Densitometry of the uncleaved band in each lane from A) is shown. The experiment was repeated three times and a single representative is shown. C) Schematic of the GFP protein and its cleavage positions.

We next assessed whether there was a correlation between potency against parasite and recombinant PMV and *P. falciparum* viability using an assay platform described previously [44]. Briefly, *P. falciparum* infected human erythrocytes were incubated with compounds for 72 h and parasite viability was then determined as a measure of LDH activity (monitored by the consumption of NADH). The results are summarized in Table 1. The *P. falciparum* viability data show a strong correlation with the PMV inhibitory activity, in that the analogues that possess the greatest inhibitory activity, against recombinant PMV and in *P. falciparum* PEXEL cleavage assays, are the most potent in reducing parasite viability. For example, P_3 Arg analogues **8**, **14**, **19-21** and **23-26** that possess PMV IC_{50} values greater than 1 μM don't exhibit parasite activity at the highest concentration tested, while P_3 Arg analogues **13**, **17** and **18** are the most potent against PMV and exhibit the greatest anti-parasitic activity (EC_{50} 1.0, 1.2 and 1.8 μM). The data also shows that the P_3 Cav analogues **27-29** are between 10- and 25-fold more potent (EC_{50} 91, 68 and 182 nM) than the comparator P_3 Arg analogues **17**, **18** and **13** (EC_{50} 1.2, 1.8 and 1.0 μM), which is consistent with activity observed in literature between **1** and **2** (EC_{50} 4.0 μM versus 0.43 μM respectively) (Fig 1 and Table 1) [36, 37]. Furthermore, **27** and **28** are 5- to 6-fold more potent (EC_{50} 0.09 and 0.07 μM) at killing *P. falciparum* parasite than our previously most potent compound, **2** (EC_{50} 0.43 μM).

To assess whether the activity observed in the *P. falciparum* parasite assay was specific to the parasite and not broadly cytotoxic to human cells, we assessed each analogue in a HepG2 cell growth inhibition assay. In this assay, we used Cell Titer-Glo as a metabolic marker of cell growth following previously described protocols [44]. The results of this assay show that only compounds **17**, **21** and **22** exhibit growth inhibition (EC_{50} 37, 35 and 24 μM) at the highest concentration tested (Table 1). This activity was deemed to be promiscuous, given there was no observable relationship

between the activities of compounds in the parasite and the cell growth inhibition assay. Notably, analogues **27** and **28** that possess the most potent anti-parasitic activity, were inactive at the highest concentration against HepG2 cells, demonstrating that these compounds are not broadly cytotoxic.

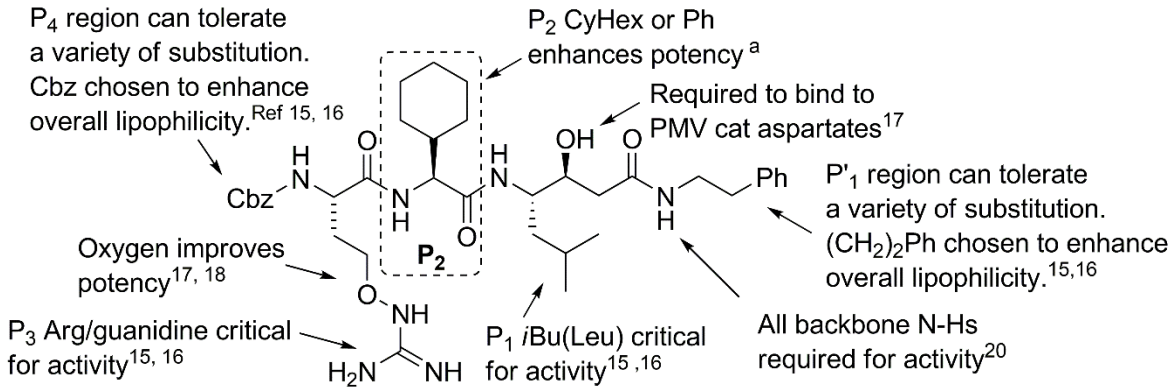

Figure 5. Overview of the structure activity relationship of the peptidomimetic inhibitors of PMV from past studies (referenced in the figure) and the study here.[a]

CONCLUSIONS

In summary of the work presented here, we have explored the P_2 region using the scaffold of pre-existing peptidomimetic inhibitors of PMV (**1** and **2**) as a template and demonstrated that the P_2 region is sensitive to change but is accepting of a larger range of functionalities. This is compared to the P_3 and P_1 region which only tolerates Arg/Cav or Leu in the respective positions (Fig 5) [34-36], thus, reinforcing the exquisite substrate selectivity profile of PMV that has been previously reported [23]. Commonly, Ala, Phe, Thr and Ser are found in the P_2 position of native PEXEL motifs of proteins known to be exported [27]. Interestingly, here we show these amino acids are not well tolerated in the P_2 position of peptidomimetics, in the context of the current scaffold. A possible explanation for this observation is that maybe the longer native peptide

substrates have a higher affinity for PMV as they engage with P_5, P_4, S_1', S_2' and S_3' sites that the peptidomimetics in this study do not, thus compensating for the tolerance of amino acids at the P_2 position of the PEXEL in native substrates.

The SAR of the analogues shown here suggests amino acids in the P_2 position that harbor disubstitution at the beta-carbon generally have the highest affinity for PMV than those without this configuration. To support this hypothesis, we found that *s*Bu **13**, CyHex **17** and Ph **18** in the P_2 position were the most optimal. This is likely due to their steric occupancy of the S_2 cavity of PMV and this was supported by the crystal structure of **27** bound to PMV. We also show that P_3 Cav orthologues **27** and **28** were several-fold more potent against PMV compared to P_3 Arg orthologues **17** and **18**. Curiously, although **13** was the most potent P_3 Arg analogue, the P_3 Cav orthologue **29** was only 2-fold more potent, and hence analogues with CyHex and Ph in the P_2 position were the focus of further biological and structural studies. Compounds **27** and **28** were also shown to have greater efficacy in preventing processing of the PEXEL containing protein PfEMP3 and reducing the viability of *P. falciparum* asexual stage parasites *in vitro*, than any PMV inhibitor previously reported. In conclusion, we have shown the modification of P_2 position has led to potent inhibitors of PMV, and thus this work will serve as a template for the future development of PMV inhibitors with improved drug-like properties with the aim to enhance *in vitro* parasite potency, and potentially efficacy in *in vivo* models of malaria.

EXPERIMENTAL SECTION

Chemistry Experimental

General

Solvents were obtained commercially and used without further purification. Analytical thin-layer chromatography was performed on Merck silica gel $^{60}F_{254}$ aluminum-backed plates and were visualized by fluorescence quenching under UV light or by $KMnO_4$ staining. Chromatography was performed with silica gel 60 (particle size 0.040-0.063 μm) using an automated purification system. NMR spectra were recorded on a Bruker Avance DRX 300 or an Agilent MR400 400 MHz or an Agilent DD2 500 MHz at 298K unless otherwise specified. Chemical shifts are reported in ppm on the δ scale and referenced to the appropriate solvent peak. MeOD and $CDCl_3$ contain H_2O.

LCMS were recorded either on a Waters LCMS system composed of a Waters 3100 Mass Detector, Waters 2996 Diode Array Detector, Waters 2545 Binary Pump, Waters SFO System Fluidics Organizer and a Waters 2767 Sample Manager (Method A), or an Agilent LCMS system composed of an Agilent G6120B Mass Detector, 1260 Infinity G1312B Binary pump, 1260 Infinity G1367E HiPALS autosampler and 1260 Infinity G4212B Diode Array Detector (Method B). Conditions for LCMS Method A were as follows, column: Kinetex TM XB-C18 5μm 4.6 x 50mm, injection volume 10 μL, 5-100% B over 3 min (solvent A: water 0.1% formic acid; solvent B: AcCN 0.1% formic acid), flow rate: 1.5 mL/min, detection: 100-600 nm, acquisition time: 6 min. Conditions for LCMS Method B were as follows, column: Poroshell 120 EC-C18, 2.1 x 50mm 2.7 Micron at 20 ºC, injection volume 2 μL, gradient: 5-100% B over 3 min (solvent A: water 0.1% formic acid; solvent B: AcCN 0.1% formic acid), flow rate: 0.8 mL/min, detection: 254 nm, acquisition time: 5 min. HPLC conditions used to assess purity of final compounds were as follows, column: Phenomenex Gemini C18, 2.0 x 50 mm; injection volume 20 μL; gradient: 0-100% Buffer B over 6 min (buffer A: 0.1% formic acid in autoclaved MilliQ water; buffer B: 0.1%

formic acid in 100% acetonitrile), flow rate: 1.0 mL/min, detection: 214 or 224 nm. Unless otherwise noted, all compounds were found to be >95% pure by this method.

HRMS were acquired by Jason Dang at the Monash Institute of Pharmaceutical Sciences Spectrometry Facility using an Agilent 1290 infinity 6224 TOF LCMS. Column used was RRHT 2.1 x 50 mm 1.8 μm C18. Gradient was applied over the 5 min with the flow rate of 0.5 mL/min. For MS: Gas temperature was 325ºC; drying gas 11 L/min; nebulizer 45 psig and the fragmentor 125V.

HCl.NH_2-Sta-$NH(CH_2)_2Ph$, Cbz-Orn(N-Boc)-Ala-OEt, Boc-Val-Sta-$NH(CH_2)_2Ph$, Cbz-Cav(*N*-Boc)-OH were synthesised using previously described protocols [36, 37]. All other amino acid building blocks were purchased from commercial vendors. All amino acid derivatives are L-configured unless otherwise stated.

Synthesis

General Procedure D

Cbz-Arg-Val-Sta-$NH(CH_2)_2Ph$.TFA (11). A mixture of Cbz-Arg(*N,N*-diBoc)-Val-Sta-$NH(CH_2)_2Ph$ (**68**) (44 mg, 0.050 mmol), in a mixture of TFA (0.5 mL) and DCM (0.5 mL) was allowed to stir for 18 h at 20 °C. The reaction mixture was concentrated to dryness *in vacuo*. The crude material was dissolved in 1:1 MeOH:H_2O (10 mL) and K_2CO_3 (100 mg, 0.724 mmol) was added. The reaction mixture was stirred for 1 h at 20 ºC. MeOH was removed *in vacuo* and extracted into EtOAc (3 x 15 mL). The organic layers were combined and washed with water (20 mL) and brine (20 mL), dried with $MgSO_4$ and evaporated to dryness *in vacuo* to give a residue. The residue was dissolved in 1:9 MeOH:TFA (5 mL) and the solution evaporated to dryness *in vacuo* to give Cbz-Arg-Val-Sta-$NH(CH_2)_2Ph$ (**11**) (9 mg, 26%). ^{1}H-NMR (300 MHz; MeOD, rotamers): δ 7.40-7.17 (m, 10H), 5.33 (s, 1H), 5.12 (m, 2H), 4.25-4.12 (m, 2H), 4.00-3.93 (m, 1H),

3.69-3.57 (m, 1H), 3.44-3.36 (m, 2H), 3.22-3.16 (m, 2H), 2.83-2.72 (m, 3H), 2.35-2.23 (m, 2H), 1.92-1.45 (m, 7H), 1.01-0.89 (m, 12H). ^{13}C-NMR (75 MHz; MeOD, rotamers) δ 173.8, 173.1, 172.6, 172.3, 172.2, 170.2, 169.7, 157.2, 139.1, 138.9, 128.4, 128.3, 128.1, 128.1, 127.7, 127.7, 127.5, 127.5, 126.0, 125.9, 69.9, 69.7, 66.5, 66.4, 59.5, 59.5, 58.2, 54.8, 54.4, 51.6, 48.1, 48.1, 48.1, 48.0, 48.0, 48.0, 48.0, 47.8, 47.8, 47.8, 47.8, 47.7, 47.5, 47.5, 47.5, 47.5, 47.5, 47.4, 47.4, 47.2, 47.2, 47.2, 47.2, 47.2, 47.1, 47.1, 40.9, 40.7, 40.6, 40.2, 39.9, 38.8, 37.0, 35.1, 34.9, 33.4, 31.6, 30.3, 29.6, 29.3, 29.3, 29.0, 28.8, 28.8, 24.8, 24.4, 23.9, 22.3, 21.1, 21.1, 20.9, 18.6, 18.3, 17.3, 16.8, 13.0. MS (Method B), *m/z* = 668 $[M + H]^+$. HRMS found: $[M + H]^+$ 668.4127; $C_{35}H_{53}N_7O_6$ requires $[M + H]^+$, 668.413.

Cbz-Arg-Ala-Sta-NH(CH$_2$)$_2$Ph.TFA (8). General procedure D was followed using Cbz-Arg(*N,N*-diBoc)-Ala-Sta-NH(CH$_2$)$_2$Ph (**69**) (39 mg, 0.046 mmol) to give Cbz-Arg-Ala-Sta-NH(CH$_2$)$_2$Ph.TFA (**8**) (13 mg, 36%). ^{1}H-NMR (300 MHz, MeOD, rotamers): δ 8.29-8.26 (m, 1H), 7.52-7.45 (m, 1H), 7.45-7.17 (m, 10H), 5.16-5.07 (m, 2H), 4.35-4.28 (m, 1H), 4.18-4.13 (m, 1H), 4.01-3.90 (m, 2H), 3.46-3.36 (m, 2H), 3.21-3.15 (m, 2H), 2.81 (t, *J* = 7.4 Hz, 2H), 2.31-2.23 (m, 2H), 1.88-1.23 (m, 10H), 0.93-0.87 (m, 6H). ^{13}C-NMR (75 MHz, MeOD, rotamers) δ 173.7, 173.6, 172.8, 172.6, 157.2, 139.1, 136.6, 128.4, 128.1, 128.1, 127.7, 127.5, 125.9, 70.0, 66.5, 54.4, 51.2, 49.7, 48.4, 48.2, 47.9, 47.6, 47.3, 47.0, 46.7, 40.7, 40.6, 40.2, 40.1, 35.1, 28.9, 24.7, 24.4, 22.3, 21.0, 16.7. MS (Method B), *m/z* = 640 $[M + H]^+$. HRMS found: $[M + H]^+$ 640.3817; $C_{33}H_{49}N_7O_6$ requires $[M + H]^+$, 640.3820.

Cbz-Arg-Abu-Sta-NH(CH$_2$)$_2$Ph.TFA (9). General procedure D was followed using Cbz-Arg(*N,N*-diBoc)-Abu-Sta-NH(CH$_2$)$_2$Ph (**70**) (12 mg, 0.014 mmol) to give Cbz-Arg-Abu-Sta-NH(CH$_2$)$_2$Ph.TFA (**9**) (3 mg, 28%). ^{1}H-NMR (300 MHz, MeOD, rotamers): δ 8.45 (br s, 1H), 7.40-7.17 (m, 10H), 5.12 (d, *J* = 1.5 Hz, 2H), 4.25-4.16 (m, 2H), 4.01-3.91 (m, 2H), 3.46-3.37 (m,

2H), 3.22-3.16 (m, 2H), 2.81 (t, *J* = 7.5 Hz, 2H), 2.25 (d, *J* = 6.4 Hz, 2H), 1.92-1.81 (m, 2H), 1.79-1.51 (m, 6H), 1.39-1.30 (m, 1H), 1.00 (t, *J* = 7.4 Hz, 3H), 0.93-87 (m, 6H). ^{13}C-NMR (75 MHz; MeOD, rotamers): δ 173.1, 172.9, 172.6, 157.2, 139.1, 128.4, 128.1, 127.7, 127.5, 125.9, 100.0, 69.9, 66.4, 55.5, 54.4, 51.3, 48.4, 48.1, 47.9, 47.6, 47.3, 47.0, 46.7, 40.7, 40.6, 40.2, 40.0, 39.0, 35.1, 28.9, 25.0, 24.7, 24.4, 22.3, 20.9, 9.5. MS (Method A), *m/z* = 654 $[M + H]^+$. HRMS found: $[M + H]^+$ 654.3977; $C_{34}H_{51}N_7O_6$; requires [M + H]+, 654.3974.

Cbz-Arg-Nva-Sta-NH(CH$_2$)$_2$Ph.TFA (10). General procedure D was followed using Cbz-Arg(*N,N*-diBoc)-Nva-Sta-NH(CH$_2$)$_2$Ph (**71**) (53 mg, 0.061 mmol) to obtain Cbz-Arg-Nva-Sta-NH(CH$_2$)$_2$Ph.TFA (**10**) as a solid (44 mg, 92%). ^{1}H-NMR (300 MHz; MeOD, rotamers): δ 7.55–7.15 (m, 10H), 5.16–5.05 (m, 2H), 4.35–4.22 (m, 1H), 4.22–4.11 (m, 1H), 4.03–3.85 (m, 2H), 3.45–3.35 (m, 2H), 3.25–3.07 (m, 2H), 2.80 (t, *J* = 7.5 Hz, 2H), 2.25 (d, *J* = 6.6 Hz, 2H), 1.87–1.48 (m, 8H), 1.48–1.30 (m, 3H), 1.01–0.80 (m, 9H). ^{13}C-NMR (75 MHz; MeOD, rotamers): δ 174.7, 174.7, 174.1, 158.8, 140.7, 138.2, 135.0, 129.9, 129.6, 129.6, 129.2, 129.0, 127.5, 71.6, 68.0, 56.1, 55.5, 52.8, 42.2, 42.1, 41.8, 41.6, 36.7, 35.2, 30.9, 30.4, 26.3, 26.0, 23.9, 22.5, 20.4, 14.1. MS (Method B), *m/z* = 668 $[M+H]^+$. HRMS found: $[M + H]^+$ 668.4140; $C_{35}H_{53}N_7O_6$ requires $[M + H]^+$, 668.4130.

Cbz-Arg-Leu-Sta-NH(CH$_2$)$_2$Ph.TFA (12). General procedure D was followed using Cbz-Arg(*N,N*-diBoc)-Leu-Sta-NH(CH$_2$)$_2$Ph (**72**) (32 mg, 0.035 mmol) to give Cbz-Arg-Leu-Sta-NH(CH$_2$)$_2$Ph.TFA (**12**) (18 mg, 65%). ^{1}H-NMR (300 MHz, MeOD, rotamers): δ 7.72-7.16 (m, 10H), 5.16-5.06 (m, 2H), 4.42-4.32 (m, 1H), 4.22-4.12 (m, 1H), 4.01-3.90 (m, 2H), 3.49-3.35 (m, 2H), 3.24-3.14 (m, 2H), 2.81 (t, *J* = 8.5 Hz, 2H), 2.32-2.18 (m, 2H), 1.90-1.49 (m, 9H), 1.43-1.07 (m, 1H), 1.03-0.65 (m, 12H). ^{13}C-NMR (75 MHz, MeOD, rotamers): δ 173.4, 173.2, 172.6, 172.1, 157.2, 139.1, 136.6, 128.4, 128.1, 127.7, 127.5, 125.9, 72.7, 70.1, 66.5, 54.6, 52.5, 51.3, 48.4, 48.2,

47.9, 47.6, 47.3, 47.0, 46.7, 42.5, 40.7, 40.6, 40.2, 40.1, 35.1, 31.6, 29.3, 28.8, 24.8, 24.5, 24.4, 22.3, 22.1, 20.9, 20.4, 13.0. MS (Method B), *m/z* = 682 $[M + H]^+$. HRMS found: $[M + H]^+$ 682.4284; $C_{36}H_{55}N_7O_6$ requires $[M + H]^+$, 682.4287.

Cbz-Arg-Ile-Sta-NH(CH$_2$)$_2$Ph.TFA (13). General procedure D was followed using Cbz-Arg(*N,N*-diBoc)-Ile-Sta-NH(CH$_2$)$_2$Ph (**73**) (44 mg, 0.049 mmol) to obtain Cbz-Arg-Ile-Sta-NH(CH$_2$)$_2$Ph.TFA (**13**) as a solid (36 mg, 92%). ^{1}H-NMR (300 MHz; MeOD, rotamers): δ 7.38-7.14 (m, 10H), 5.09 (s, 2H), 4.25-4.10 (m, 2H), 4.01–3.87 (m, 2H), 3.47-3.33 (m, 2H), 3.17 (t, *J* = 6.5 Hz, 2H), 2.79 (t, *J* = 7.4 Hz, 2H), 2.29-2.19 (m, 2H), 1.93-1.73 (m, 2H), 1.71-1.47 (m, 6H), 1.30-1.38 (m, 1H), 1.27-1.10 (m, 1H), 1.02–0.79 (m, 12H). ^{13}C-NMR (75 MHz; MeOD, rotamers): δ 174.7, 174.1, 173.9, 173.8, 173.8, 162.2, 161.8, 158.8, 158.8, 158.7, 140.6, 138.2, 129.9, 129.6, 129.2, 129.0, 127.5, 71.5, 68.0, 60.2, 56.1, 53.1, 42.2, 42.1, 41.7, 41.4, 37.9, 36.7, 30.9, 30.9, 30.4, 26.4, 26.1, 26.0, 23.9, 22.4, 16.3, 11.5. MS (Method B), *m/z* = 682 $[M+H]^+$. HRMS found: $[M + H]^+$ 682.4297; $C_{36}H_{55}N_7O_6$ requires $[M + H]^+$, 682.4287.

Cbz-Arg-tBuGly-Sta-NH(CH$_2$)$_2$Ph.TFA (14). General procedure D was followed using Cbz-Arg(*N,N*-diBoc)-tBuGly-Sta-NH(CH$_2$)$_2$Ph (**74**) (39 mg, 0.046 mmol) to give Cbz-Arg-tBuGly-Sta-NH(CH$_2$)$_2$Ph.TFA (**14**) (14 mg, 37%). ^{1}H-NMR (300 MHz, MeOD): δ 8.45 (s, 1H), 7.42-7.17 (m, 10H), 5.11 (s, 2H), 4.25-4.21 (m, 2H), 4.00-3.91 (m, 2H), 3.46-3.36 (m, 2H), 3.23-3.15 (m, 2H), 2.81 (t, *J* = 7.4 Hz, 2H), 2.32-2.21 (m, 2H), 1.88-1.80 (m, 1H), 1.73-1.48 (m, 5H), 1.39-1.30 (m, 1H), 1.04 (s, 9H), 0.91 (dd, *J* = 12.9 and 6.4 Hz, 6H). ^{13}C-NMR (75 MHz; MeOD): δ 172.8, 172.6, 171.2, 157.2, 157.1, 139.1, 136.6, 128.4, 128.1, 127.7, 127.5, 125.9, 70.0, 66.4, 61.5, 54.4, 51.6, 48.4, 48.2, 47.9, 47.6, 47.3, 47.0, 46.7, 40.7, 40.6, 40.2, 39.6, 39.0, 33.5, 28.7, 25.9, 24.9, 24.5, 22.3, 20.9. MS (Method B), *m/z* = 682 $[M + H]^+$. HRMS found: $[M + H]^+$ 682.4285; $C_{36}H_{55}N_7O_6$ requires $[M + H]^+$, 682.4287.

Cbz-Arg-EtNva-Sta-NH(CH$_2$)$_2$Ph.TFA (15). General procedure D was followed using Cbz-Arg(*N,N*-diBoc)-EtNva-Sta-NH(CH$_2$)$_2$Ph (**75**) (68 mg, 0.075 mmol) to give Cbz-Arg-EtNva-Sta-NH(CH$_2$)$_2$Ph.TFA (**15**) (27 mg, 45%). ^{1}H-NMR (300 MHz, MeOD, rotamers): δ 8.52 (br s, 1H), 7.42-7.17 (m, 10H), 5.16-5.07 (m, 2H), 4.43 (d, *J* = 6.6 Hz, 1H), 4.24-4.17 (m, 1H), 4.01-3.91 (m, 2H), 3.49-3.35 (m, 2H), 3.23-3.14 (m, 2H), 2.81 (t, *J* = 7.4 Hz, 2H), 2.25 (d, *J* = 6.3 Hz, 2H), 1.86-1.33 (m, 12H), 0.97-0.78 (m, 12H). ^{13}C-NMR (75 MHz, MeOD, rotamers): δ 173.3, 172.6, 168.3, 157.2, 157.1, 139.1, 136.7, 128.4, 128.1, 127.7, 127.5, 125.9, 69.9, 66.4, 55.6, 54.5, 51.5, 48.4, 48.2, 47.9, 47.6, 47.3, 47.0, 46.7, 42.5, 40.7, 40.6, 40.2, 39.9, 39.0, 35.1, 28.6, 24.9, 24.5, 22.3, 21.7, 21.0, 20.9, 10.2, 9.8. MS (Method B), *m/z* = 696 [M + H]$^+$. HRMS found: [M + H]$^+$ 696.4449; $C_{37}H_{57}N_7O_6$ requires [M + H]$^+$, 696.4443.

Cbz-Arg-CyPenGly-Sta-NH(CH$_2$)$_2$Ph.TFA (16). General procedure D was followed using Cbz-Arg(*N,N*-diBoc)-CyPenGly-Sta-NH(CH$_2$)$_2$Ph (**76**) (26 mg, 0.029 mmol) to give Cbz-Arg-CyPenGly-Sta-NH(CH$_2$)$_2$Ph.TFA (**16)** (18 mg, 79%). ^{1}H-NMR (300 MHz, MeOD, rotamers): δ 7.39-7.17 (m, 10H), 5.11 (s, 2H), 4.21-4.14 (m, 2H), 4.00-3.90 (m, 2H), 3.47-3.37 (m, 2H), 3.21-3.15 (m, 2H), 2.81 (t, *J* = 7.4 Hz, 2H), 2.27-2.22 (m, 3H), 1.88-1.21 (m, 15H), 0.93-0.86 (m, 6H). ^{13}C-NMR (75 MHz, MeOD, rotamers): δ 172.9, 172.7, 172.6, 157.2, 157.0, 139.1, 136.6, 128.4, 128.1, 127.7, 127.5, 125.9, 70.0, 66.4, 58.1, 54.3, 51.4, 48.4, 48.2, 47.9, 47.6, 47.3, 47.0, 46.7, 41.6, 40.7, 40.6, 40.2, 39.9, 35.1, 31.6, 29.3, 29.1, 28.9, 24.9, 24.8, 24.6, 24.4, 22.4, 20.9, 13.0. MS (Method B), *m/z* = 694 [M + H]$^+$. HRMS found: [M + H]$^+$ 694.4292; $C_{37}H_{55}N_7O_6$ requires [M + H]$^+$, 694.4287.

Cbz-Arg-CyHexGly-Sta-NH(CH$_2$)$_2$Ph.TFA (17). General procedure D was followed using Cbz-Arg(*N,N*-diBoc)-CyHexGly-Sta-NH(CH$_2$)$_2$Ph (**77**) (39 mg, 0.046 mmol) to give Cbz-Arg-CyHexGly-Sta-NH(CH$_2$)$_2$Ph.TFA (**17**) (14 mg, 37%). ^{1}H-NMR (300 MHz, MeOD, rotamers):

δ 7.40-7.17 (m, 10H), 5.12 (s, 2H), 4.22-4.14 (m, 2H), 4.00-3.90 (m, 2H), 3.47-3.37 (m, 2H), 3.21-3.15 (m, 2H), 2.81 (t, *J* = 7.4 Hz, 2H), 2.26-2.24 (m, 2H), 1.87-1.49 (m, 11H), 1.39-1.00 (m, 7H), 0.95-0.88 (m, 6H). ^{13}C-NMR (75 MHz, MeOD, rotamers): δ 173.0, 172.6, 172.1, 159.5, 159.0, 157.2, 157.1, 139.1, 136.6, 128.4, 128.1, 127.7, 127.4, 125.9, 117.5, 113.7, 69.9, 66.4, 58.9, 54.4, 51.6, 48.4, 48.2, 47.9, 47.6, 47.3, 47.0, 46.7, 40.7, 40.6, 40.1, 39.7, 39.6, 35.1, 29.6, 28.9, 28.5, 25.8, 25.7, 25.6, 24.8, 24.5, 22.3, 20.9. MS (Method B), *m/z* = 708 $[M + H]^+$. HRMS found: $[M + H]^+$ 708.4456; $C_{38}H_{57}N_7O_6$ requires $[M + H]^+$, 708.4443.

Cbz-Arg-Phg-Sta-NH(CH$_2$)$_2$Ph.TFA (18). General procedure D was followed using Cbz-Arg(*N,N*-diBoc)-Phg-Sta-NH(CH$_2$)$_2$Ph (**78**) (17 mg, 0.019 mmol) to obtain Cbz-Arg-Phg-Sta-NH(CH$_2$)$_2$Ph.TFA (**18**) as a solid (14 mg, 93%). ^{1}H-NMR (300 MHz; MeOD, rotamers): δ d 7.51–7.38 (m, 2H), 7.38–7.14 (m, 13H), 5.46–5.37 (m, 1H), 5.09 (s, 2H), 4.27–4.14 (m, 1H), 3.99–3.85 (m, 2H), 3.38–3.33 (m, 2H), 3.17 (t, *J* = 6.6 Hz, 2H), 2.75 (t, *J* = 7.37 Hz, 2H), 2.07–1.78 (m, 3H), 1.76–1.50 (m, 5H), 1.38–1.30 (m, 1H), 0.90 (d, *J* = 7.5 Hz, 3H), 0.88 (d, *J* = 7.5 Hz, 3H). ^{13}C-NMR (75 MHz; MeOD, rotamers): δ 174.2, 174.1, 172.7, 172.6, 158.8, 140.6, 138.5, 130.0, 130.0, 129.7, 129.6, 129.2, 129.0, 128.9, 127.5, 71.5, 68.0, 59.4, 55.9, 53.2, 53.1, 42.2, 42.1, 41.5, 41.4, 36.6, 30.9, 30.4, 26.3, 26.0, 23.8, 22.5. MS (Method B), *m/z* = 702 $[M + H]^+$. HRMS found: $[M + H]^+$ 702.3974; $C_{38}H_{51}N_7O_6$ requires $[M + H]^+$, 702.3974.

Cbz-Arg-Phe-Sta-NH(CH$_2$)$_2$Ph.TFA (19). General procedure D was followed using Cbz-Arg(*N,N*-diBoc)-Phe-Sta-NH(CH$_2$)$_2$Ph (**79**) (80 mg, 0.087 mmol) to obtain Cbz-Arg-Phe-Sta-NH(CH$_2$)$_2$Ph.TFA (**19**) (68 mg, 94%) as a solid. ^{1}H-NMR (300 MHz; MeOD, rotamers): δ 7.40–7.14 (m, 15H), 5.18-5.01 (m, 2H), 4.70–4.63 (m, 1H), 4.09 (t, *J* = 6.7 Hz, 1H), 3.98–3.86 (m, 2H), 3.48–3.36 (m, 2H), 3.23–3.06 (m, 3H), 3.03–2.91 (m, 1H), 2.81 (t, *J* = 7.4 Hz, 2H), 2.19- 1.98 (m, 2H), 1.79–1.45 (m, 6H), 1.45–1.20 (m, 1H), 0.94–0.87 (m, 6H). ^{13}C-NMR (75 MHz; MeOD,

rotamers): δ 174.1, 173.9, 173.2, 158.5, 140.3, 138.1, 137.8, 130.2, 129.6, 129.4, 129.4, 129.0, 128.7, 127.7, 127.2, 71.0, 67.8, 56.2, 56.0, 52.7, 41.9, 41.8, 41.2, 41.1, 38.5, 36.4, 30.0, 25.9, 25.6, 23.6, 22.3. MS (Method B), *m/z* = 716 $[M + H]^+$. HRMS found: $[M + H]^+$ 716.4128; $C_{39}H_{53}N_7O_6$ requires $[M + H]^+$, 716.4130.

Cbz-Arg-β-phenyl-Phe-Sta-NH(CH$_2$)$_2$Ph.TFA (20). General procedure D was followed using Cbz-Arg(*N,N*-diBoc)-β-phenyl-Phe-Sta-NH(CH$_2$)$_2$Ph (**80**) (61 mg, 0.062 mmol) to obtain Cbz-Arg-β-phenyl-Phe-Sta-NH(CH$_2$)$_2$Ph.TFA (**20**) as a solid (55 mg, 99%). ^{1}H-NMR (300 MHz; MeOD, rotamers): δ 7.39–7.10 (m, 19H), 7.05–6.97 (m, 1H), 5.39 (d, *J* = 11.4 Hz, 1H), 5.08–4.95 (m, 2H), 4.43 (d, *J* = 11.7 Hz, 1H), 4.03–3.93 (m, 1H), 3.76–3.62 (m, 2H), 3.42–3.34 (m, 2H), 3.05 (t, *J* = 6.6 Hz, 2H), 2.83–2.74 (m, 2H), 1.63–1.32 (m, 8H), 1.25–1.13 (m, 1H), 0.88–0.72 (m, 6H). ^{13}C-NMR (75 MHz; MeOD, rotamers): δ 174.3, 173.9, 172.5, 162.9, 162.5, 158.8, 158.7, 142.4, 142.2, 140.6, 138.0, 130.0, 129.9, 129.8, 129.7, 129.7, 129.6, 129.5, 129.2, 129.0, 128.2, 128.0, 127.6, 71.3, 68.0, 57.6, 56.2, 54.6, 52.8, 42.0, 41.9, 41.4, 41.1, 36.5, 30.4, 26.1, 25.7, 23.9, 22.4. MS (Method B), *m/z* = 792 $[M + H]^+$. HRMS found: $[M + H]^+$ 792.4457; $C_{45}H_{57}N_7O_6$ requires $[M + H]^+$, 792.4443.

Cbz-Arg-β-methyl-Phe-Sta-NH(CH$_2$)$_2$Ph.TFA (21). General procedure D was followed using Cbz-Arg(*N,N*-diBoc)-β-methyl-Phe-Sta-NH(CH$_2$)$_2$Ph (**81**) (70 mg, 0.075 mmol) to obtain Cbz-Arg-β-methyl-Phe-Sta-NH(CH$_2$)$_2$Ph.TFA (**21**) as a solid (63 mg, 99%). ^{1}H-NMR (300 MHz; MeOD, rotamers): δ 7.38–7.03 (m, 15H), 5.10–4.96 (m, 2H), 4.58 (d, *J* = 9.0 Hz, 1H), 3.99–3.92 (m, 2H), 3.77–3.53 (m, 1H), 3.49–3.33 (m, 2H), 3.28–3.16 (m, 1H), 3.14–2.96 (m, 2H), 2.84–2.71 (m, 2H), 2.30–2.20 (m, 2H), 1.60–1.22 (m, 10H), 0.93–0.85 (m, 6H). ^{13}C-NMR (75 MHz; MeOD, rotamers): δ 174.1, 174.1, 173.3, 162.3, 161.8, 158.7, 158.5, 143.6, 140.6, 138.0, 129.9, 129.8, 129.7, 129.6, 129.3, 129.0, 128.1, 127.5, 73.7, 72.6, 71.5, 68.1, 62.3, 60.4, 56.3, 53.2, 43.9, 42.8,

42.2, 42.0, 41.8, 41.2, 36.7, 30.0, 26.2, 25.9, 23.9, 22.4, 19.9. MS (Method B), *m/z* = 730 [M + H]$^+$. HRMS found: [M + H]$^+$ 730.4284; $C_{40}H_{55}N_7O_6$ requires [M + H]$^+$, 730.4287.

Cbz-Arg-2-indanylgly-Sta-NH(CH$_2$)$_2$Ph.TFA (22). General procedure D was followed using Cbz-Arg(*N,N*-diBoc)-2-indanylgly-Sta-NH(CH$_2$)$_2$Ph (**82**) (91 mg, 0.097 mmol) to obtain Cbz-Arg-2-indanylgly-Sta-NH(CH$_2$)$_2$Ph.TFA (**22**) as a solid (80 mg, 97%). ^{1}H-NMR (300 MHz; MeOD, rotamers): δ 7.41–7.01 (m, 14H), 5.43- 5.30 (m, 0.4H), 5.16–5.01 (m, 2H), 4.49–4.38 (m, 1H), 4.24–4.06 (m, 1H), 4.06–3.91 (m, 1H), 3.69–3.53 (m, 0.6H), 3.46–3.33 (m, 2H), 3.26–3.12 (m, 2H), 3.09–2.70 (m, 8H), 2.35–2.19 (m, 1H), 1.89–1.49 (m, 6H), 1.41–1.28 (m, 1H), 1.04–0.83. (m, 6H). ^{13}C-NMR (75 MHz; MeOD, rotamers): δ 173.8, 173.1, 172.6, 172.2, 170.0, 169.7, 161.1, 160.7, 157.3, 142.0, 141.8, 141.5, 139.1, 138.9, 136.6, 136.5, 128.4, 128.3, 128.1, 128.1, 127.8, 127.7, 127.5, 126.3, 126.1, 126.0, 124.0, 70.1, 66.6, 57.6, 56.6, 55.0, 54.6, 51.7, 51.5, 41.6, 40.9, 40.7, 40.6, 40.3, 39.8, 38.8, 37.0, 35.7, 35.5, 35.1, 34.9, 28.8, 28.7, 25.0, 24.9, 24.5, 23.9, 22.4, 21.3, 21.2, 21.0. MS (Method B), *m/z* = 742 [M + H]$^+$. HRMS found: [M + H]$^+$ 742.4295; $C_{41}H_{55}N_7O_6$ requires [M + H]+, 742.4287.

Cbz-Arg-Ser-Sta-NH(CH$_2$)$_2$Ph.TFA (23). General procedure D was followed using Cbz-Arg(*N,N*-diBoc)-Ser-Sta-NH(CH$_2$)$_2$Ph (**83**) (20 mg, 0.0234 mmol) to obtain Cbz-Arg-Ser-Sta-NH(CH$_2$)$_2$Ph.TFA (**23**) as a solid (17 mg, 95%). ^{1}H-NMR (300 MHz; MeOD, rotamers): δ d 7.45–7.11 (m, 10H), 5.16–5.06 (m, 2H), 4.38 (t, *J* = 4.8 Hz, 1H), 4.24–4.11 (m, 1H), 4.03–3.91 (m, 2H), 3.86–3.77 (m, 1H), 3.39 (t, *J* = 7.6 Hz, 2H), 3.25–3.12 (m, 2H), 2.79 (t, *J* = 7.5 Hz, 2H), 2.32-2.22 (m, 2H), 1.92–1.80 (m, 1H), 1.76–1.56 (m, 4H), 1.56–1.48 (m, 1H), 1.41–1.25 (m, 2H), 0.98–0.81 (m, 6H). ^{13}C-NMR (75 MHz; MeOD, rotamers): δ 174.4, 173.9, 172.1, 158.5, 152.2, 140.4, 129.7, 129.4, 129.4, 129.0, 128.8, 127.2, 71.2, 67.8, 62.8, 57.0, 55.9, 52.6, 42.0, 41.9, 41.6, 41.4, 36.4,

30.6, 30.1, 26.0, 25.7, 23.5, 22.3. MS (Method B), *m/z* = 656 $[M + H]^+$. HRMS found: $[M + H]^+$ 656.3761; $C_{33}H_{49}N_7O_7$ requires $[M + H]^+$, 656.3766.

Cbz-Arg-(S)-β-hydroxy-Val-Sta-NH(CH$_2$)$_2$Ph.TFA (24). General procedure D was followed using Cbz-Arg(*N,N*-diBoc)-β-hydroxy-Val-Sta-NH(CH$_2$)$_2$Ph (**84**) (18 mg, 0.020 mmol) to obtain Cbz-Arg-β-hydroxy-Val-Sta-NH(CH$_2$)$_2$Ph.TFA (**24**) as a solid (13 mg, 82%). ^{1}H-NMR (300 MHz; MeOD, rotamers): δ 7.52–7.14 (m, 10H), 5.17–5.03 (m, 2H), 4.34–4.16 (m, 2H), 3.96 (t, *J* = 5.6 Hz, 2H), 3.45–3.34 (m, 2H), 3.24–3.11 (m, 2H), 2.84–2.73 (m, 2H), 2.33–2.21 (m, 2H), 1.92–1.77 (m, 1H), 1.77 –1.45 (m, 5H), 1.38–1.20 (m, 7H), 0.92 (d, *J* = 6.6 Hz, 3H), 0.89 (d, *J* = 6.8 Hz, 3H). ^{13}C-NMR (75 MHz; MeOD, rotamers): δ 174.8, 174.5, 174.2, 172.4, 158.8, 140.7, 129.9, 129.7, 129.7, 129.3, 129.1, 129.0, 127.5, 72.3, 72.1, 71.6, 68.0, 62.8, 56.1, 53.1, 53.0, 42.3, 42.1, 41.9, 41.6, 36.7, 30.9, 30.2, 28.1, 26.8, 26.4, 26.0, 23.9, 22.5, 22.4. MS (Method B), *m/z* = 684 $[M + H]^+$. HRMS found: $[M + H]^+$ 684.4073; $C_{35}H_{53}N_7O_7$ requires $[M + H]^+$, 684.4079.

Cbz-Arg-Thr-Sta-NH(CH$_2$)$_2$Ph.TFA (25). General procedure D was followed using Cbz-Arg(*N,N*-diBoc)-Thr-Sta-NH(CH$_2$)$_2$Ph (**85**) (50 mg, 0.058 mmol) to obtain Cbz-Arg-Thr-Sta-NH(CH$_2$)$_2$Ph.TFA (**25**) as a solid (41 mg, 91%). ^{1}H-NMR (300 MHz; MeOD, rotamers): δ 7.41–7.15 (m, 10H), 5.13 (s, 2H), 4.32 (d, *J* = 3.3 Hz, 1H), 4.28–4.17 (m, 2H), 4.04–3.92 (m, 2H), 3.46–3.36 (m, 2H), 3.20 (t, *J* = 6.6 Hz, 2H) 2.81 (t, *J* = 7.48 Hz, 2H), 2.29 (d, *J* = 6.6 Hz, 2H), 1.98–1.83 (m, 1H), 1.83–1.48 (m, 5H), 1.42–1.29 (m, 1H), 1.22 (d, *J* = 6.4 Hz, 3H), 0.95–0.88 (m, 6H). ^{13}C-NMR (75 MHz; MeOD, rotamers): δ 175.0, 174.1, 172.6, 158.8, 140.7, 129.9, 129.7, 129.6, 129.2, 129.0, 127.5, 71.5, 68.5, 68.1, 60.5, 56.3, 52.9, 42.3, 42.1, 41.9, 41.6, 36.7, 30.2, 26.4, 25.9, 23.8, 22.6, 20.7. MS (Method B), *m/z* = 670 $[M+H]^+$. HRMS found: $[M + H]^+$ 670.3914; $C_{34}H_{51}N_7O_7$; requires $[M + H]^+$, 670.3923.

Cbz-Arg-D,L-*threo*-β-phenyl-Ser-Sta-NH(CH$_2$)$_2$Ph.TFA (26). General procedure D was followed using Cbz-Arg(*N,N*-diBoc)-*threo*-β-phenyl-Ser-Sta-NH(CH$_2$)$_2$Ph (**86**) (58 mg, 0.062 mmol) to obtain Cbz-Arg-*threo*-β-phenyl-Ser-Sta-NH(CH$_2$)$_2$Ph.TFA (**26**) as a solid (50 mg, 95%). ^{1}H-NMR (300 MHz; MeOD, rotamers): δ 7.47–7.13 (m, 15H), 5.28 (dd, *J* = 3.5, 18.3 Hz, 1H), 5.20–4.98 (m, 2H), 4.61 (d, *J* = 4.0 Hz, 1H), 4.14–3.88 (m, 3H), 3.47–3.35 (m, 2H), 3.12–2.95 (m, 2H), 2.80 (t, *J* = 7.5 Hz, 2H), 2.41–2.29 (m, 1H), 2.20–2.08 (m, 1H), 1.66–1.49 (m, 3H), 1.47–1.25 (m, 4H), 0.93–0.87 (m, 3H), 0.84 (d, *J* = 6.4 Hz, 3H). ^{13}C-NMR (75 MHz; MeOD, rotamers): δ 175.0, 174.7, 174.2, 174.2, 172.3, 172.2, 162.2, 161.7, 158.7, 158.5, 142.9, 142.8, 140.7, 140.6, 138.1, 138.0, 129.9, 129.9, 129.7, 129.6, 129.5, 129.3, 129.2, 129.0, 129.0, 128.8, 128.8, 127.5, 127.5, 127.4, 127.4, 73.7, 73.6, 71.8, 71.5, 68.2, 68.0, 61.6, 61.2, 56.5, 56.4, 53.0, 52.9, 42.3, 42.2, 42.1, 42.0, 41.8, 41.6, 41.4, 41.0, 36.7, 36.6, 29.9, 29.7, 26.1, 26.0, 25.8, 25.7, 23.9, 23.9, 22.6, 22.5. MS (Method B), *m/z* = 732 [M + H]$^+$. HRMS found: [M + H]+ 732.4077; C39H53N7O7 requires [M + H]+, 732.4079.

Cbz-Cav(NH$_2$)-CyHexGly-Sta-NH(CH$_2$)$_2$Ph.TFA (27). General procedure D was followed using Cbz-Cav(N-Boc)-CyHexGly-Sta-NH(CH$_2$)$_2$Ph (**87**) (75 mg, 0.093 mmol) to obtain Cbz-Cav(NH$_2$)-CyHexGly-Sta-NH(CH$_2$)$_2$Ph.TFA (**27**) as a solid (69 mg, 90%). ^{1}H-NMR (300 MHz; MeOD, rotamers): δ 7.39–7.13 (m, 10H), 5.11 (s, 2H), 4.42–4.31 (m, 1H), 4.19 (d, *J* = 7.26 Hz, 1H), 4.01–3.87 (m, 4H), 3.49–3.34 (m, 2H), 2.84–2.74 (m, 2H), 2.29–2.09 (m, 3H), 2.07–1.89 (m, 1H), 1.81–1.47 (m, 8H), 1.40-1.01 (m, 6H), 0.95–0.82 (m, 6H). ^{13}C-NMR (75 MHz; MeOD, rotamers): δ 174.2, 174.1, 173.6, 161.5, 161.0, 160.6, 158.7, 140.6, 138.1, 129.9, 129.7, 129.6, 129.3, 129.0, 127.5, 74.7, 71.4, 68.1, 60.4, 53.5, 53.1, 42.2, 41.6, 41.3, 36.7, 31.7, 31.1, 30.0, 27.3, 27.2, 27.1, 26.0, 23.9, 22.4. MS (Method B), *m/z* = 710 [M+H]$^+$. HRMS found: [M + H]$^+$ 710.4244; $C_{37}H_{55}N_7O_7$ requires [M + H]$^+$, 710.4236.

Cbz-Cav(NH_2)-Phg-Sta-$NH(CH_2)_2Ph$.TFA (28). General procedure D was followed using Cbz-Cav(N-Boc)-Phg-Sta-$NH(CH_2)_2Ph$ (**88**) (34 mg, 0.042 mmol) to obtain Cbz-Cav(NH_2)-Phg-Sta-$NH(CH_2)_2Ph$.TFA (**28**) as a solid (23 mg, 67%). ^{1}H-NMR (300 MHz; MeOD, rotamers): δ 7.46 (d, *J* = 5.9 Hz, 2H), 7.41–7.23 (m, 10H), 7.23–7.13 (m, 3H), 5.46 (s, 1H), 5.11 (s, 2H), 4.46–4.32 (m, 1H), 4.02–3.86 (m, 4H), 3.39–3.34 (m, 2H), 2.76 (t, *J* = 7.4 Hz, 2H), 2.30–2.12 (m, 1H), 2.12–1.86 (m, 3H), 1.72–1.48 (m, 2H), 1.41–1.21 (m, 1H), 0.92 (d, *J* = 6.8 Hz, 3H), 0.90 (d, *J* = 6.6 Hz, 3H). ^{13}C-NMR (75 MHz; MeOD, rotamers): δ 174.1, 173.8, 172.5, 160.7, 158.7, 140.6, 138.6, 130.1, 129.9, 129.7, 129.7, 129.6, 129.3, 129.0, 128.9, 127.5, 74.7, 71.4, 68.1, 59.2, 53.5, 53.1, 42.1, 41.4, 41.4, 36.6, 31.7, 26.0, 23.8, 22.5. MS (Method B), *m/z* = 704 $[M+H]^+$. HRMS found: $[M + H]^+$ 704.3776; $C_{37}H_{49}N_7O_7$ requires $[M + H]^+$, 704.3766.

Cbz-Cav(NH_2)-Ile-Sta-$NH(CH_2)_2Ph$.TFA (29). General procedure D was followed using Cbz-Cav(N-Boc)-Ile-Sta-$NH(CH_2)_2Ph$ (**89**) (10 mg, 0.013 mmol) to obtain TFA.Cbz-Cav(NH_2)-Ile-Sta-$NH(CH_2)_2Ph$ as a solid (9 mg, 88%). ^{1}H-NMR (300 MHz; MeOD, rotamers): δ 7.39 – 7.14 (m, 10H), 5.11 (s, 2H), 4.40 – 4.31 (m, 1H), 4.21 (d, *J* = 7.7 Hz, 1H), 4.01 – 3.89 (m, 4H), 3.46 – 3.36 (m, 2H), 2.84 – 2.74 (m, 2H), 2.29 – 2.20 (m, 2H), 2.19 – 2.09 (m, 1H), 2.05 – 1.92 (m, 1H), 1.89 – 1.80 (m, 1H), 1.65 – 1.47 (m, 3H), 1.31 - 1.39 (m, 1H), 1.26 – 1.10 (m, 1H), 1.04 - 0.78 (m, 12H). HRMS found: $[M + H]^+$ 684.4082; $C_{35}H_{53}N_7O_7$ requires $[M + H]^+$, 684.4079.

General Procedure A

Boc-Leu-Sta-$NH(CH_2)_2Ph$ (30). A mixture of HCl.NH_2-Sta-$NH(CH_2)_2Ph$ (50 mg, 0.158 mmol), Boc-Leu-OH (35 mg, 0.151 mmol), HBTU (75 mg, 0.196 mmol) and DIPEA (194 µL, 1.11 mmol) in DMF (2 mL) was allowed to stir for 18 h at 20 ºC. The reaction mixture was quenched with 10% citric acid solution (1 x 10 mL) and the desired product extracted into EtOAc (3 x 15 mL). The organic layers were combined, washed with saturated $NaHCO_3$ (1 x 20 mL) and brine (1 x 20

mL), dried with $MgSO_4$ and concentrated *in vacuo* to obtain the crude residue. The crude residue was purified using a silica chromatography gradient eluting from 100% DCM to 10% MeOH/DCM to obtain Boc-Leu-NH$(CH_2)_2$Ph (**30**) (46 mg, 59%). ^{1}H-NMR (500 MHz; $CDCl_3$, rotamers): δ 7.32 (t, *J* = 7.4 Hz, 2H), 7.26-7.20 (m, 3H), 6.67-6.52 (m, 1H), 6.38-6.32 (m, 1H), 4.79 (s, 1H), 4.03-3.97 (m, 2H), 3.84-3.78 (m, 1H), 3.62-3.55 (m, 1H), 3.55-3.48 (m, 1H), 2.87-2.83 (m, 2H), 2.55-2.47 (m, 1H), 2.21 (d, *J* = 13.9 Hz, 1H), 1.71-1.54 (m, 5H), 1.44 (s, 9H), 1.38-1.25 (m, 2H), 0.96 (dd, *J* = 8.6 and 6.3 Hz, 6H), 0.90 (t, *J* = 6.6 Hz, 6H). MS (Method B), *m/z* = 492 $[M + H]^+$.

Boc-Abu-Sta-NH$(CH_2)_2$Ph (31). General procedure A was followed using Boc-Abu-OH (46 mg, 0.224 mmol) and HCl.NH_2-Sta-NH$(CH_2)_2$Ph (50 mg, 0.159 mmol) to obtain Boc-Abu-NH$(CH_2)_2$Ph (**31**) (53 mg, 66%). ^{1}H-NMR (300 MHz; $CDCl_3$, rotamers): δ 7.33-7.19 (m, 5H), 6.77 (br s, 1H), 6.53-6.49 (m, 1H), 5.10-5.08 (m, 1H), 4.00-3.85 (m, 3H), 3.55-3.44 (m, 2H), 2.83 (t, *J* = 7.3 Hz, 2H), 2.38-2.22 (m, 2H), 1.87-1.56 (m, 4H), 1.43 (s, 9H, overlap with adjacent multiplet) 1.41-1.23 (m, 11H), 0.97 (t, *J* = 7.4 Hz, 3H), 0.90 (d, *J* = 5.2 Hz, 6H). MS (Method A), *m/z* = 464 $[M + H]^+$.

Boc-Nva-Sta-NH$(CH_2)_2$Ph (32). General procedure A was followed using Boc-Nva-OH (38 mg, 0.175 mmol) and HCl.NH_2-Sta-NH$(CH_2)_2$Ph (50 mg, 0.159 mmol) to obtain Boc-Nva-NH$(CH_2)_2$Ph (**32**) as a solid (57 mg, 75%). ^{1}H-NMR (300 MHz; $CDCl_3$, rotamers): δ 7.35–7.28 (m, 2H), 7.27–7.18 (m, 3H), 6.27 (d, *J* = 9.0 Hz, 1H), 6.19–6.07 (m, 1H), 4.93–4.80 (m, 1H), 4.34 (br s, 1H), 4.03–3.90 (m, 2H), 3.90–3.76 (m, 1H), 3.62–3.41 (m, 2H), 2.87–2.79 (m, 2H), 2.47–2.31 (m, 1H), 2.23–2.08 (m, 1H), 1.86–1.69 (m, 1H), 1.64–1.49 (m, 3H), 1.44 (s, 9H), 1.41–1.29 (m, 3H), 1.01–0.84 (m, 9H). MS (Method B), *m/z* = 478 $[M+H]^+$.

Boc-Ile-Sta-NH$(CH_2)_2$Ph (33). General procedure A was followed using Boc-Ile-OH (40 mg, 0.175 mmol) and HCl.NH_2-Sta-NH$(CH_2)_2$Ph (50 mg, 0.159 mmol) to obtain Boc-Ile-NH$(CH_2)_2$Ph

(**33**) as an oil (62 mg, 79%). ^{1}H-NMR (300 MHz; $CDCl_3$, rotamers): δ 7.37–7.29 (m, 2H), 7.28–7.19 (m, 3H), 6.29–6.09 (m, 2H), 4.90 (d, *J* = 7.7 Hz, 1H), 4.39 (d, *J* = 3.1 Hz, 1H), 4.05–3.93 (m, 1H), 3.88–3.75 (m, 2H), 3.65–3.41 (m, 2H), 2.90–2.76 (m, 2H), 2.50–2.33 (m, 1H), 2.22–2.10 (m, 1H), 1.99–1.81 (m, 1H), 1.66–1.47 (m, 3H), 1.45 (s, 9H), 1.43–1.33 (m, 1H), 1.23–1.04 (m, 1H), 0.99–0.89 (m, 12H). MS (Method B), *m/z* = 492 $[M + H]^+$.

Boc-tBuGly-Sta-NH$(CH_2)_2$Ph (34). General procedure A was followed using Boc-tBuGly-OH (48 mg, 0.206 mmol) and HCl.NH_2-Sta-NH$(CH_2)_2$Ph (50 mg, 0.159 mmol) to obtain Boc-tBuGly-NH$(CH_2)_2$Ph (**34**) (26 mg, 33%). ^{1}H-NMR (300 MHz; $CDCl_3$): δ 7.35-7.21 (m, 5H), 6.25 (br s, 1H), 5.89 (d, *J* = 8.7 Hz, 1H), 5.03 (d, *J* = 7.9 Hz, 1H), 4.38 (br s, 1H), 4.01-3.96 (m, 1H), 3.82-3.44 (m, 4H), 2.86-2.80 (m, 2H), 2.44-2.37 (m, 1H), 2.16-2.11 (m, 1H), 1.59-1.52 (m, 2H), 1.43 (s, 9H), 1.42-1.33 (m, 1H), 1.03 (s, 9H), 0.90 (d, *J* = 6.3 Hz, 6H). MS (Method B), *m/z* = 492 $[M + H]^+$.

Boc-EtNva-Sta-NH$(CH_2)_2$Ph (35). General procedure A was followed using Boc-EtNva-OH (57 mg, 0.233 mmol) and HCl.NH_2-Sta-NH$(CH_2)_2$Ph (57 mg, 0.179 mmol) to obtain Boc-EtNva-NH$(CH_2)_2$Ph (**35**) (49 mg, 54%). ^{1}H-NMR (300 MHz; $CDCl_3$, rotamers): δ 7.36-7.20 (m, 5H), 6.39-6.33 (m, 1H), 6.19 (br s, 1H), 4.84-4.78 (m, 1H), 4.11-4.06 (m, 1H), 4.03-3.97 (m, 1H), 3.92-3.84 (m, 1H), 3.60-3.46 (m, 2H), 2.86-2.81 (m, 2H), 2.48-2.37 (m, 1H), 2.21-2.13 (m, 1H), 1.82 (br s, 1H), 1.66-1.47 (m, 3H), 1.45 (s, 9H), 1.42-1.15 (m, 4H), 0.98-0.87 (m, 12H). MS (Method A), *m/z* = 506 $[M + H]^+$.

Boc-CyPenGly-Sta-NH$(CH_2)_2$Ph (36). Boc-L-CyPenGly.DHCA (121 mg, 0.286 mmol) was dissolved in EtOAc (20 mL) and washed with 10% citric acid (20 mL) and brine (20 mL). The organic layer was dried with anhydrous $MgSO_4$, filtered and evaporated to give Boc-CyPenGly-OH (70 mg, 0.286 mmol, 99% recovery). General procedure A was followed using Boc-

CyPenGly-OH (70 mg, 0.233 mmol) and HCl.NH_2-Sta-$NH(CH_2)_2Ph$ (102 mg, 0.324 mmol) to obtain Boc-CyPenGly-$NH(CH_2)_2Ph$ (**36**) (57 mg, 39%). ^{1}H-NMR (300 MHz, $CDCl_3$, rotamers): δ 7.36- 7.21 (m, 5H), 6.49 (br s, 1H), 6.21-6.15 (m, 1H), 4.94-4.90 (m, 1H), 4.02-3.96 (m, 1H), 3.76 (t, *J* = 7.5 Hz, 2H), 3.67-3.43 (m, 2H), 2.89-2.83 (m, 2H), 2.53-2.40 (m, 1H), 2.27-2.14 (m, 3H), 1.67-1.56 (m, 7H), 1.45 (s, 9H), 1.40-1.27 (m, 4H), 0.91 (dd, *J* = 6.4 and 3.0 Hz, 6H). MS (Method B), *m/z* = 504 $[M + H]^+$.

Cbz-CyHexGly-Sta-$NH(CH_2)_2Ph$ (37). General procedure A was followed using Cbz-CyHexGly-OH (60 mg, 0.206 mmol) and HCl.NH_2-Sta-$NH(CH_2)_2Ph$ (50 mg, 0.159 mmol) to obtain Cbz-CyHexGly-$NH(CH_2)_2Ph$ (**37**) (30 mg, 34%). ^{1}H-NMR (300 MHz; $CDCl_3$, rotamers): δ 7.42-7.18 (m, 10H), 6.29-6.17 (m, 2H), 5.32-5.27 (m, 1H), 5.12-5.04 (m, 2H), 4.33 (br s, 1H), 4.02-3.78 (m, 3H), 3.63-3.43 (m, 2H), 2.84 (t, *J* = 6.1 Hz, 2H), 2.38-2.29 (m, 1H), 2.18-2.11 (m, 1H), 1.87-1.50 (m, 7H), 1.41-0.98 (m, 7H), 0.90 (d, *J* = 5.3 Hz, 6H). MS (Method B), *m/z* = 552 $[M + H]^+$.

Boc-Phg-Sta-$NH(CH_2)_2Ph$ (38). General procedure A was followed using Boc-Phg-OH (48 mg, 0.191 mmol) and HCl.NH_2-Sta-$NH(CH_2)_2Ph$ (**38**) (60 mg, 0.191 mmol) to obtain Boc-Phg-Sta-$NH(CH_2)_2Ph$ as a solid (73 mg, 75%). ^{1}H-NMR (300 MHz; $CDCl_3$, rotamers): δ 7.40–7.28 (m, 6H), 7.27–7.15 (m, 4H), 6.42 (d, *J* = 7.3 Hz, 1H), 6.00 (br s, 1H), 5.67 (br s, 1H), 5.07 (d, *J* = 5.3 Hz, 1H), 4.26 (s, 1H), 3.99–3.79 (m, 2H), 3.55–3.30 (m, 2H), 2.77 (t, *J* = 7.0 Hz, 2H), 2.01–1.83 (m, 2H), 1.76–1.48 (m, 2H), 1.46–0.98 (m, 10H), 0.94–0.81 (m, 6H). MS (Method B), *m/z* = 512 $[M + H]^+$.

Boc-Phe-Sta-$NH(CH_2)_2Ph$ (39). General procedure A was followed using Boc-Phe-OH (42 mg, 0.159 mmol) and HCl.NH_2-Sta-$NH(CH_2)_2Ph$ (50 mg, 0.159 mmol) to obtain Boc-Phe-Sta-$NH(CH_2)_2Ph$ (**39**) as a solid (66 mg, 79%). ^{1}H-NMR (300 MHz; $CDCl_3$, rotamers): δ 7.36–7.29

(m, 2H), 7.26–7.12 (m, 8H), 6.17 (d, *J* = 9.5 Hz, 1H), 6.01 (t, *J* = 5.5 Hz, 1H), 4.93 (d, *J* = 7.3 Hz, 1H), 4.29 (q, *J* = 6.9 Hz, 1H), 4.12 (br. s., 1H), 3.95–3.87 (m, 1H), 3.80 (d, *J* = 4.6 Hz, 1H), 3.63–3.39 (m, 2H), 3.05 (d, *J* = 7.04 Hz, 2H), 2.87–2.77 (m, 2H), 2.02–1.94 (m, 2H), 1.57–1.46 (m, 2H), 1.41 (s, 9H), 1.32–1.25 (m, 1H), 0.91–0.85 (m, 6H). MS (Method B), *m/z* = 526 $[M + H]^+$.

Boc-β-phenyl-Phe-Sta-NH(CH$_2$)$_2$Ph (40). General procedure A was followed using Boc-β-phenyl-Phe-OH (65 mg, 0.191 mmol) and HCl.NH$_2$-Sta-NH(CH$_2$)$_2$Ph (60 mg, 0.191 mmol) to obtain Boc-β-phenyl-Phe-Sta-NH(CH$_2$)$_2$Ph (**40**) as a solid (86 mg, 75%). ^{1}H-NMR (300 MHz; CDCl$_3$, rotamers): δ 7.40–7.27 (m, 9H), 7.26–7.10 (m, 6H), 7.01–6.92 (m, 1H), 6.09 (d, *J* = 9.2 Hz, 1H), 5.67 (t, *J* = 6.1 Hz, 1H), 4.92 (d, *J* = 8.8 Hz, 1H), 4.82 (t, *J* = 9.4 Hz, 1H), 4.46 (d, *J* = 10.1 Hz, 1H), 3.90–3.76 (m, 2H), 3.68 (s, 1H), 3.63–3.40 (m, 2H), 2.83 (t, *J* = 6.6 Hz, 2H), 1.62–1.39 (m, 3H), 1.36 (s, 9H), 1.33–1.16 (m, 1H), 0.85 (d, *J* = 2.2 Hz, 3H), 0.83 (d, *J* = 2.2 Hz, 3H). MS (Method B), *m/z* = 602 $[M + H]^+$.

Boc-β-methyl-Phe-NH(CH$_2$)$_2$Ph (41). General procedure A was followed using (2*S*,3*S*)-Boc-β-methyl-Phe-OH (34 mg, 0.121 mmol) and HCl.NH$_2$-Sta-NH(CH$_2$)$_2$Ph (38 mg, 0.121 mmol) to obtain Boc-β-methyl-Phe-NH(CH$_2$)$_2$Ph (**41**) as an oil (60 mg, 92%). ^{1}H-NMR (300 MHz; CDCl$_3$, rotamers): ^{1}H-NMR (300 MHz; CDCl$_3$, rotamers): δ 7.41–7.27 (m, 5H), 7.27–7.15 (m, 5H), 6.30–6.17 (m, 1H), 6.12 (d, *J* = 9.5 Hz, 1H), 4.73 (d, *J* = 7.0 Hz, 1H), 4.27 (d, *J* = 2.9 Hz, 1H), 4.20–4.10 (m, 1H), 4.00–3.88 (m, 1H), 3.88–3.74 (m, 1H), 3.65–3.36 (m, 3H), 2.91–2.74 (m, 2H), 2.43–2.24 (m, 1H), 2.21–2.09 (m, 1H), 1.53–1.42 (m, 2H), 1.39 (s, 9H), 1.36 (d, *J* = 7.04 Hz, 3H), 1.32–1.23 (m, 1H), 0.92–0.83 (m, 6H). MS (Method B), *m/z* = 540 $[M + H]^+$.

Boc-2-indanylgly-Sta-NH(CH$_2$)$_2$Ph (42). General procedure A was followed using Boc-2-indanylgly-OH (51 mg, 0.175 mmol) and HCl.NH$_2$-Sta-NH(CH$_2$)$_2$Ph (55 mg, 0.175 mmol) to

obtain Boc-2-indanylgly-Sta-NH(CH_2)$_2$Ph (**42**) as a solid (94 mg, 98%). ^{1}H-NMR (300 MHz; $CDCl_3$, rotamers): δ 7.32–7.27 (m, 2H), 7.27–7.14 (m, 7H), 6.20 (d, *J* = 9.7 Hz, 1H), 6.15–6.05 (m, 1H), 4.94 (d, *J* = 6.6 Hz, 1H), 4.32 (d, *J* = 2.6 Hz, 1H), 4.00 (t, *J* = 7.3 Hz, 2H), 3.86–3.74 (m, 1H), 3.67–3.54 (m, 1H), 3.54-3.42 (m, 1H), 3.11–2.99 (m, 2H), 2.97–2.75 (m, 6H), 2.48–2.34 (m, 1H), 2.20–2.09 (m, 1H), 1.68–1.63 (m, 1H), 1.43 (s, 9H), 1.38 (t, *J* = 5.1 Hz, 1H), 0.93 (d, *J* = 1.3 Hz, 3H), 0.91 (d, *J* = 1.3 Hz, 3H). MS (Method B), *m/z* = 552 $[M + H]^+$.

Boc-Ser-Sta-NH(CH_2)$_2$Ph (43). General procedure A was followed using Boc-Ser-OH (33 mg, 0.159 mmol) and HCl.NH_2-Sta-NH(CH_2)$_2$Ph (50 mg, 0.159 mmol) to obtain Boc-Ser-Sta-NH(CH_2)$_2$Ph (**43**) as an oil (64 mg, 74%). ^{1}H-NMR (300 MHz; $CDCl_3$, rotamers): δ 7.33–7.27 (m, 2H), 7.25–7.16 (m, 3H), 6.86 (d, *J* = 8.8 Hz, 1H), 6.65–6.55 (m, 1H), 5.64 (d, *J* = 6.6 Hz, 1H), 4.58 (br s, 1H), 4.24–4.06 (m, 1H), 4.00–3.85 (m, 3H), 3.85–3.61 (m, 2H), 3.58–3.33 (m, 2H), 2.80 (t, *J* = 7.3 Hz, 2H), 2.45–2.33 (m, 1H), 2.28–2.18 (m, 1H), 1.72–1.52 (m, 2H), 1.49–1.41 (m, 9H), 1.41–1.14 (m, 1H), 0.92–0.87 (m, 6H). MS (Method B), *m/z* = 466$[M + H]^+$.

Fmoc-β-hydroxy-Val-Sta-NH(CH_2)$_2$Ph (44). General procedure A was followed using Fmoc-β-hydroxy-Val-OH (43 mg, 0.121 mmol) and HCl.NH_2-Sta-NH(CH_2)$_2$Ph (38 mg, 0.121 mmol) to obtain Fmoc-β-hydroxy-Val-Sta-NH(CH_2)$_2$Ph (**44**) as an oil (52 mg, 70%). ^{1}H-NMR (300 MHz; $CDCl_3$, rotamers): δ 7.77 (d, *J* = 7.5 Hz, 2H), 7.58 (d, *J* = 7.48 Hz, 2H), 7.45–7.37 (m, 2H), 7.35–7.28 (m, 4H), 7.27–7.13 (m, 3H), 6.43 (d, *J* = 9.2 Hz, 1H), 6.11–6.00 (m, 1H), 5.82 (d, *J* = 8.8 Hz, 1H), 4.45–4.31 (m, 3H), 4.26–4.08 (m, 2H), 4.01–3.89 (m, 2H), 3.88–3.79 (m, 1H), 3.60–3.43 (m, 2H), 2.86–2.76 (m, 2H), 2.41–2.25 (m, 1H), 2.25–2.12 (m, 1H), 1.63–1.49 (m, 2H), 1.38–1.20 (m, 7H), 0.87–0.73 (m, 6H). MS (Method B), *m/z* = 616 $[M + H]^+$.

Boc-Thr-Sta-NH(CH_2)$_2$Ph (45). General procedure A was followed using Boc-Thr-OH (35 mg, 0.159 mmol) and HCl.NH_2-Sta-NH(CH_2)$_2$Ph (50 mg, 0.159 mmol) to obtain Boc-Thr-Sta-

$NH(CH_2)_2Ph$ (**45**) as a solid (57 mg, 75%). ^{1}H-NMR (300 MHz; $CDCl_3$, rotamers): δ 7.34-7.27 (m, 2H), 7.26–7.17 (m, 3H), 6.72 (d, *J* = 9.7 Hz, 1H), 6.41–6.33 (m, 1H), 5.53 (d, *J* = 7.9 Hz, 1H) 4.47 (br s, 1H), 4.36-4.20 (m, 1H), 4.08–3.94 (m, 2H), 3.94–3.81 (m, 1H), 3.64–3.35 (m, 3H), 2.81 (t, *J* = 7.2 Hz, 2H), 2.43–2.27 (m, 1H), 2.28–2.16 (m, 1H), 1.98 (br s, 1H), 1.67–1.49 (m, 1H), 1.45 (s, 9H), 1.24–1.40 (m, 1H), 1.24–1.16 (m, 3H), 0.92–0.86 (m, 6H). MS (Method B), *m/z* = 480 $[M + H]^+$.

Boc-D,L-*threo*-β-phenyl-Ser-Sta-$NH(CH_2)_2Ph$ (47). General procedure A was followed using Boc-D,L-*threo*-β-phenyl-Ser-OH (49 mg, 0.175 mmol) and HCl.NH_2-Sta-$NH(CH_2)_2Ph$ (55 mg, 0.175 mmol) to obtain Boc-*threo*-β-phenyl-Ser-Sta-$NH(CH_2)_2Ph$ (**47**) as an oil (63 mg, 67%). ^{1}H-NMR (300 MHz; $CDCl_3$, rotamers): δ 7.41–7.28 (m, 7H), 7.27–7.16 (m, 3H), 6.66 (d, *J* = 9.7 Hz, 1H), 6.22 (t, *J* = 5.8 Hz, 0.5H), 6.01 (t, *J* = 5.8 Hz, 0.5H), 5.26-5.44 (m, 2H), 4.39–4.23 (m, 2H), 4.03–3.82 (m, 2H), 3.76 (d, *J* = 3.3 Hz, 1H), 3.63–3.42 (m, 3H), 2.86–2.76 (m, 2H), 2.40–2.06 (m, 2H), 1.62–1.47 (m, 2H), 1.39–1.27 (m, 9H), 0.96–0.82 (m, 6H). MS (Method B), *m/z* = 542 $[M + H]^+$.

General Procedure B

Cbz-Orn(N-Boc)-Leu-Sta-$NH(CH_2)_2Ph$ (48). A mixture of Boc-Leu-Sta-$NH(CH_2)_2Ph$ (**29**) (37 mg, 0.074 mmol) and 4M HCl in dioxane was stirred for 1 h at 20 ºC. The reaction mixture was concentrated to dryness *in vacuo* to obtain the crude residue as a on oil. A mixture of the crude residue, Cbz-Orn(N-Boc)-OH (33 mg, 0.089 mmol), HBTU (40 mg, 0.104 mmol) and DIPEA (93 µL, 0.523 mmol) was allowed to stir in DMF (1 mL) for 18 h. The reaction mixture was quenched with 10% citric acid solution (1 x 10 mL) and the desired product extracted into EtOAc (3 x 15 mL). The organic layers were combined, washed with saturated $NaHCO_3$ (1 x 20 mL) and brine (1 x 20 mL), dried with $MgSO_4$, filtered and concentrated *in vacuo* to obtain the crude residue. The

crude residue was purified using a silica chromatography gradient eluting from 100% DCM to 10% MeOH/DCM to obtain Cbz-Orn(N-Boc)-Leu-NH(CH_2)$_2$Ph (**48**) (58 mg). ^{1}H-NMR (400 MHz; $CDCl_3$, rotamers): δ 7.49-7.06 (m, 10H), 6.82-6.73 (m, 1H), 5.99-5.91 (m, 1H), 5.05 (s, 2H), 4.32-4.24 (m, 2H), 4.00-3.91 (m, 1H), 3.91-3.84 (m, 1H), 3.79-3.70 (m, 1H), 3.67-3.58 (m, 1H), 3.56-3.33 (m, 2H), 3.17 (br s, 1H), 3.12-2.97 (m, 2H), 2.92 (d, *J* = 5.3 Hz, 1H), 2.79 (t, *J* = 7.3 Hz, 2H), 2.36-2.12 (m, 3H), 1.78 (br s, 2H), 1.64-1.46 (m, 5H), 1.46 (s, 9H), 1.32-1.06 (m, 3H), 0.98-0.69 (m, 12H). MS (Method B), *m/z* = 740 $[M + H]^+$.

Cbz-Orn(N-Boc)-Ala-Sta-NH(CH_2)$_2$Ph (49). A mixture of Cbz-Orn(N-Boc)-Ala-OEt (80 mg, 0.172 mmol) and LiOH hydrate (18 mg, 0.430 mmol) in a mixture of water (0.8 mL) and THF (2.4 mL) was allowed to stir for 3 h at 20 ºC. The reaction was quenched with 10% citric acid (1 x10 mL) and the aqueous layer extracted with EtOAc (3 x 15 mL). The organic layers were combined and washed with brine (20 mL), dried with anhydrous $MgSO_4$, filtered and concentrated *in vacuo* to obtain an oil. The oil was dissolved in DMF (2 mL) and DIPEA (170 µL, 0.953 mmol), HBTU (62 mg, 0.163 mmol) and HCl.NH_2-Sta-NH(CH_2)$_2$Ph (43 mg, 0.136 mmol) was added. The mixture was then stirred for 18 h at 20 ºC. The reaction was quenched with 10% citric acid (10 mL) and the mixture extracted with EtOAc (3 x 15 mL). The organic layers were combined, washed with saturated $NaHCO_3$ (20 mL) and brine (20 mL), dried with anhydrous $MgSO_4$ and concentrated to dryness *in vacuo* to obtain Cbz-Orn(N-Boc)-Ala-NH(CH_2)$_2$Ph (**49**) (43 mg, 45%). ^{1}H-NMR (400 MHz, $CDCl_3$): δ 7.37-6.99 (m, 10H), 7.02 (br s, 1H), 6.77 (br s, 1H), 5.93 (d, *J* = 7.4 Hz, 1H), 5.06 (s, 2H), 4.39-4.29 (m, 2H), 3.97-3.80 (m, 2H), 3.55-3.37 (m, 2H), 3.17 (s, 1H), 3.06-2.87 (m, 2H), 2.80 (t, *J* = 7.3 Hz, 2H), 2.34-2.23 (m, 2H), 1.81-1.77 (m, 1H), 1.66-1.51 (m, 5H), 1.38-1.23 (m, 13H), 0.94-0.86 (m, 6H). MS (Method B), *m/z* = 698 $[M + H]^+$.

Cbz-Orn(N-Boc)-Abu-Sta-NH(CH_2)$_2$Ph (50). General procedure B was followed using Boc-Abu-Sta-NH(CH_2)$_2$Ph (**31**) (53 mg, 0.113 mmol) and Cbz-Orn(N-Boc)-OH (52 mg, 0.148 mmol) to obtain Cbz-Orn(N-Boc)-Abu-Sta-NH(CH_2)$_2$Ph (**50**) (12 mg, 14%). ^{1}H-NMR (300 MHz; $CDCl_3$): δ 7.40- 7.08 (m, 10H), 6.69 (br s, 1H), 6.56 (br s, 1H), 5.87-5.79 (m, 1H), 5.10 (s, 2H), 4.94 (br s, 1H), 4.32 (br s, 1H), 4.22 (m, 1H), 4.01-3.93 (m, 1H), 3.93-3.82 (m, 2H), 3.61-3.39 (m, 2H), 3.24-3.05 (m, 3H), 2.81 (t, *J* = 7.3 Hz, 2H), 2.39-2.15 (m, 2H), 1.89-1.10 (m, 18H), 1.01-0.70 (m, 9H). MS (Method B), *m/z* = 712 $[M + H]^+$.

Cbz-Orn(N-Boc)-Nva-Sta-NH(CH_2)$_2$Ph (51). General procedure B was followed using Boc-Nva-Sta-NH(CH_2)$_2$Ph (**32**) (57 mg, 0.120 mmol) and Cbz-Orn(N-Boc)-OH (43 mg, 0.118 mmol) to obtain Cbz-Orn(N-Boc)-Nva-Sta-NH(CH_2)$_2$Ph (**51**) as a solid (47 mg, 54%). ^{1}H-NMR (300 MHz; $CDCl_3$, rotamers): δ 7.36–7.27 (m, 6H), 7.26–7.15 (m, 4H), 6.94–6.55 (m, 2H), 5.93–5.78 (m, 1H), 5.08 (s, 2H), 5.01–4.87 (m, 1H), 4.71–4.46 (m, 1H), 4.39–4.19 (m, 2H), 4.01–3.80 (m, 2H), 3.60–3.34 (m, 2H), 3.28–2.99 (m, 2H), 2.81 (t, *J* = 7.37 Hz, 2H), 2.37–2.14 (m, 2H), 2.14–1.96 (m, 3H), 1.86–1.71 (m, 2H), 1.65–1.47 (m, 4H), 1.43 (s, 9H), 1.40–1.26 (m, 3H), 0.96–0.82 (m, 9H). MS (Method B), *m/z* = 726 $[M+H]^+$.

Cbz-Orn(N-Boc)-Val-Sta-NH(CH_2)$_2$Ph (52). A mixture of HCl.NH_2-Val-Sta-NH(CH_2)$_2$Ph (60 mg 0.117 mmol), Cbz-Orn(N-Boc)-OH (33 mg, 0.089 mmol), HBTU (40 mg, 0.104 mmol) and DIPEA (202 µL) in DMF (1 mL) was allowed to stir for 18 h at 20 ºC. The reaction mixture was quenched with 10% citric acid solution (1 x 10 mL) and the desired product extracted into EtOAc (3 x 15 mL). The organic layers were combined, washed with saturated $NaHCO_3$ (1 x 20 mL) and brine (1 x 20 mL), dried with $MgSO_4$ and concentrated *in vacuo*. The crude material was purified using a silica chromatography gradient eluting from 100% DCM to 10% MeOH/DCM to obtain

Cbz-Orn(N-Boc)-Val-NH(CH_2)$_2$Ph (**52**) (66 mg, 62%). ^{1}H NMR data was identical to that previously described.[39] MS (Method A), *m/z* = 726 $[M + H]^+$.

Cbz-Orn(N-Boc)-Ile-Sta-NH(CH_2)$_2$Ph (53). General procedure B was followed using Boc-Ile-Sta-NH(CH_2)$_2$Ph (**33**) (62 mg, 0.126 mmol) and Cbz-Orn(N-Boc)-OH (45 mg, 0.124 mmol) to obtain Cbz-Orn(N-Boc)-Ile-Sta-NH(CH_2)$_2$Ph (**53**) as a solid (74 mg, 81%). ^{1}H-NMR (300 MHz; $CDCl_3$, rotamers): δ 7.41–7.27 (m, 7H), 7.27–7.16 (m, 3H), 6.88–6.72 (m, 1H), 6.50–6.22 (m, 2H), 5.81–5.62 (m, 1H), 5.18–5.04 (m, 2H), 4.92–4.76 (m, 1H), 4.39–4.19 (m, 2H), 4.08 (t, *J* = 6.93 Hz, 1H), 4.01–3.73 (m, 2H), 3.64–3.36 (m, 2H), 3.34–2.99 (m, 2H), 2.89–2.77 (m, 2H), 2.43–2.26 (m, 1H), 2.26–2.08 (m, 1H), 2.01–1.74 (m, 2H), 1.61–1.49 (m, 5H), 1.44 (s, 9H), 1.39–1.20 (m, 2H), 1.19–1.02 (m, 1H), 1.00–0.63 (m, 12H). MS (Method B), *m/z* = 740 $[M + H]^+$.

Cbz-Orn(N-Boc)-tBuGly-Sta-NH(CH_2)$_2$Ph (54). General procedure B was followed using Boc-tBuGly-Sta-NH(CH_2)$_2$Ph (**34**) (26 mg, 0.052 mmol) and Cbz-Orn(N-Boc)-OH (27 mg, 0.075 mmol) to obtain Cbz-Orn(N-Boc)-tBuGly-Sta-NH(CH_2)$_2$Ph (**54**). ^{1}H-NMR (300 MHz, $CDCl_3$): δ 7.37-7.16 (m, 10H), 7.13-6.90 (m, 2H), 6.14-6.11 (m, 1H), 5.10 (s, 2H), 5.01-5.00 (m, 1H), 4.35-4.26 (m, 2H), 4.02-3.88 (m, 3H), 3.50-3.45 (m, 2H), 3.20-3.00 (m, 2H), 2.82 (t, *J* = 7.0 Hz, 2H), 2.39-2.26 (m, 2H), 1.89-1.08 (m, 16H), 1.00 (s, 9H), 0.92-0.71 (m, 6H). MS (Method B), *m/z* = 740 $[M + H]^+$.

Cbz-Orn(N-Boc)-EtNva-Sta-NH(CH_2)$_2$Ph (55). General procedure B was followed using Boc-EtNva-Sta-NH(CH_2)$_2$Ph (**35**) (49 mg, 0.096 mmol) and Cbz-Orn(N-Boc)-OH (44 mg, 0.126 mmol) to obtain Cbz-Orn(N-Boc)-EtNva-Sta-NH(CH_2)$_2$Ph (**55**) (62.5 mg, 86%). ^{1}H-NMR (300 MHz; $CDCl_3$): δ 7.47-7.37 (m, 1H), 7.37-7.15 (m, 10H), 7.18-7.00 (m, 2H), 6.18-6.14 (m, 1H), 5.10-5.01 (m, 3H), 4.47-4.30 (m, 2H), 3.99-3.90 (m, 2H), 3.52-3.42 (m, 2H), 3.20-3.05 (m, 2H),

2.83 (t, *J* = 7.3 Hz, 2H), 2.32-2.27 (m, 2H), 1.87-1.16 (m, 21H), 0.95-0.75 (m, 12H). MS (Method B), *m/z* = 754 $[M + H]^+$.

Cbz-Orn(N-Boc)-CyPenGly-Sta-NH(CH$_2$)$_2$Ph (56). General procedure B was followed using Boc-CyPenGly-Sta-NH(CH$_2$)$_2$Ph (**36**) (57 mg, 0.112 mmol) and Cbz-Orn(N-Boc)-OH (52 mg, 0.146 mmol) to obtain Cbz-Orn(N-Boc)-CyPenGly-Sta-NH(CH$_2$)$_2$Ph (**56**) (37 mg, 44%). ^{1}H-NMR (300 MHz, $CDCl_3$): δ 7.80 (s, 1H), 7.32-7.16 (m, 10H), 6.25 (br s, 1H), 5.05 (s, 2H), 4.95 (br s, 1H), 4.40-4.33 (m, 2H), 4.00-3.90 (m, 2H), 3.51-3.41 (m, 2H), 3.16-3.09 (m, 2H), 2.82-2.80 (m, 2H), 2.37-2.24 (m, 3H), 1.76-1.20 (m, 27H), 0.94-0.73 (m, 6H). MS (Method B), *m/z* = 752 $[M + H]^+$.

NH$_2$-CyHexGly-Sta-NH(CH$_2$)$_2$Ph (57). A mixture of Cbz-CyHexGly-Sta-NH(CH$_2$)$_2$Ph (**37**) (30 mg, 0.053 mmol) and Pd/C (cat.) (3 mg, 0.028 mmol) in EtOAc was allowed to stir under a nitrogenous atmosphere for 18 h. The mixture was filtered through Celite, rinsed with methanol and the filtrate concentrated to dryness *in vacuo*. The residue obtained was subjected to a silica chromatography gradient eluting from 100% DCM to 5% MeOH/DCM to obtain NH$_2$-CyHexGly-Sta-NH(CH$_2$)$_2$Ph (**57**) as a solid (17 mg, 75%).^{1}H-NMR (300 MHz, $CDCl_3$, rotamers): δ 7.57 (d, *J* = 10.0 Hz, 1H), 7.39-7.17 (m, 5H), 6.78 (t, *J* = 5.7 Hz, 1H), 4.02-3.85 (m, 2H), 3.60-3.37 (m, 2H), 3.24-3.10 (m, 1H), 2.89-2.74 (m, 2H), 2.41-2.09 (m, 2H), 2.02-1.84 (m, 1H), 1.77-1.00 (m, 13H), 0.96-0.69 (m, 6H). MS (Method B), *m/z* = 418 $[M + H]^+$.

Cbz-Orn(N-Boc)-CyHexGly-Sta-NH(CH$_2$)$_2$Ph (58). A mixture of NH$_2$-CyHexGly-NH(CH$_2$)$_2$Ph (**57**) (17 mg, 0.040 mmol), Cbz-Orn(N-Boc)-OH (18 mg, 0.052 mmol), HBTU (19.8 mg, 0.052 mmol) and DIPEA (50 μL, 0.281 mmol) in DMF (1 mL) was allowed to stir for 18 h. The reaction mixture was quenched with 10% citric acid solution (1 x 10 mL) and the desired product extracted into EtOAc (3 x 15 mL). The organic layers were combined, washed with

saturated $NaHCO_3$ (1 x 20 mL) and brine (1 x 20 mL), dried with $MgSO_4$, filtered and concentrated *in vacuo* to obtain the crude residue. The crude residue was purified using a silica chromatography gradient eluting from 100% DCM to 10% MeOH/DCM to obtain Cbz-Orn(N-Boc)-CyHexGly-$NH(CH_2)_2Ph$ (**58**) (35 mg, 116%, impure). ^{1}H-NMR (300 MHz, $CDCl_3$, rotamers): δ 7.56-7.15 (m, 11H), 7.11-7.03 (m, 1H), 6.12-6.06 (m, 1H), 5.07 (s, 2H), 4.93 (s, 1H), 4.40-4.20 (m, 2H), 4.01-3.86 (m, 3H), 3.56-3.39 (m, 3H), 3.15 (s, 2H), 2.83 (t, J = 7.3 Hz, 2H), 2.32 (s, 2H), 1.76-1.08 (m, 27H), 0.96-0.70 (m, 6H). MS (Method B), m/z = 766 $[M + H]^+$.

Cbz-Orn(N-Boc)-Phg-Sta-$NH(CH_2)_2Ph$ (59). General procedure B was followed using Boc-Phg-Sta-$NH(CH_2)_2Ph$ (**38**) (15 mg, 0.029 mmol) and Cbz-Orn(N-Boc)-OH (11 mg, 0.030 mmol) to obtain Cbz-Orn(N-Boc)-Phg-Sta-$NH(CH_2)_2Ph$ (**59**) as a solid (17 mg, 76%). ^{1}H-NMR (300 MHz; $CDCl_3$, rotamers): δ 7.37–7.28 (m, 10H), 7.27–7.16 (m, 5H), 6.36–6.20 (m, 1H), 6.03–5.84 (m, 1H), 5.70–5.54 (m, 1H), 5.32 (d, J = 5.7 Hz, 1H), 5.16–5.03 (m, 2H), 4.85–4.68 (m, 1H), 4.40–4.24 (m, 1H), 4.07–3.79 (m, 3H), 3.55–3.37 (m, 2H), 3.28–3.02 (m, 2H), 2.85–2.73 (m, 2H), 2.08–1.95 (m, 1H), 1.95–1.78 (m, 2H), 1.60–1.47 (m, 5H), 1.46–1.23 (m, 11H), 0.93–0.86 (m, 6H). MS (Method B), m/z = 760 $[M + H]^+$.

Cbz-Orn(N-Boc)-Phe-Sta-$NH(CH_2)_2Ph$ (60). General procedure B was followed using Boc-Phe-Sta-$NH(CH_2)_2Ph$ (**39**) (66 mg, 0.126 mmol) and Cbz-Orn(N-Boc)-OH (44 mg, 0.121 mmol) to obtain Cbz-Orn(N-Boc)-Phe-Sta-$NH(CH_2)_2Ph$ (**60**) as a solid (81 mg, 86%). ^{1}H-NMR (300 MHz; $CDCl_3$, rotamers): δ 7.42–7.27 (m, 7H), 7.27–7.14 (m, 8H), 6.93–6.77 (m, 1H), 6.41–6.16 (m, 2H), 5.79–5.63 (m, 1H), 5.10–4.97 (m, 2H), 4.84–4.73 (m, 1H), 4.54 (d, J = 6.6 Hz, 1H), 4.23–4.09 (m, 1H), 3.97–3.87 (m, 2H), 3.87–3.76 (m, 1H), 3.63–3.37 (m, 2H), 3.25–2.97 (m, 4H), 2.84 (t, J = 7.26 Hz, 2H), 2.10–1.94 (m, 2H), 1.91–1.66 (m, 2H), 1.60–1.53 (m, 1H), 1.53–1.35 (m, 12H), 1.35–1.16 (m, 1H), 0.92–0.86 (m, 6H). MS (Method B), m/z = 774 $[M + H]^+$.

Cbz-Orn(N-Boc)-β-phenyl-Phe-Sta-NH(CH_2)$_2$Ph (61). General procedure B was followed using Boc-β-phenyl-Phe-Sta-NH(CH_2)$_2$Ph (**40**) (54 mg, 0.089 mmol) and Cbz-Orn(N-Boc)-OH (33 mg, 0.089 mmol) to obtain Cbz-Orn(N-Boc)-β-phenyl-Phe-Sta-NH(CH_2)$_2$Ph (**61**) as a solid (61 mg, 80%). ^{1}H-NMR (300 MHz; $CDCl_3$, rotamers): δ 7.40–7.28 (m, 11H), 7.26–7.12 (m, 6H), 7.11–7.05 (m, 3H), 6.97–6.89 (m, 1H), 6.44–6.14 (m, 1H), 5.53–5.37 (m, 1H), 5.09–4.87 (m, 2H), 4.87–4.73 (m, 1H), 4.64 (d, *J* = 8.8 Hz, 1H), 4.27–4.14 (m, 2H), 3.85–3.70 (m, 2H), 3.58–3.37 (m, 2H), 3.05 (d, *J* = 6.2 Hz, 2H), 2.87–2.80 (m, 2H), 1.84–1.50 (m, 7H), 1.43 (s, 9H), 1.39–1.09 (m, 4H), 0.85–0.77 (m, 6H). MS (Method B), *m/z* = 850 $[M]^+$.

Cbz-Orn(N-Boc)-β-methyl-Phe-Sta-NH(CH_2)$_2$Ph (62). General procedure B was followed using Boc-β-methyl-Phe-NH(CH_2)$_2$Ph (**41**) (60 mg, 0.111 mmol) and Cbz-Orn(N-Boc)-OH (39 mg, 0.107 mmol) to obtain Cbz-Orn(N-Boc)-β-methyl-Phe-Sta-NH(CH_2)$_2$Ph (**62**) as an oil (62 mg, 73%). ^{1}H-NMR (300 MHz; $CDCl_3$, rotamers): δ 7.41–7.27 (m, 7H), 7.26–7.13 (m, 8H), 6.86–6.58 (m, 2H), 6.56–6.34 (m, 1H), 5.89 (br s, 1H), 5.11–4.96 (m, 1H), 4.96–4.74 (m, 2H), 4.42 (t, *J* = 7.0 Hz, 1H), 4.12–3.76 (m, 4H), 3.65–3.36 (m, 3H), 3.14–2.96 (m, 2H), 2.90–2.77 (m, 2H), 2.35–2.13 (m, 2H), 1.73–1.48 (m, 3H), 1.44 (s, 11H), 1.39–1.25 (m, 5H), 0.96–0.79 (m, 6H). MS (Method B), *m/z* = 788 $[M + H]^+$.

Cbz-Orn(N-Boc)-2-indanylgly-Sta-NH(CH_2)$_2$Ph (63). General procedure B was followed using Boc-2-indanylgly-Sta-NH(CH_2)$_2$Ph (**42**) (96 mg, 0.174 mmol) and Cbz-Orn(N-Boc)-OH (63 mg, 0.172 mmol) to obtain Cbz-Orn(N-Boc)-2-indanylgly-Sta-NH(CH_2)$_2$Ph (**63**) as a solid (95 mg, 68%). ^{1}H-NMR (300 MHz; $CDCl_3$, rotamers): δ 7.41–7.27 (m, 6H), 7.27–7.01 (m, 8H), 6.48–6.61 (m, 2H), 5.56 (d, *J* = 7.0 Hz, 1H), 5.08 (s, 2H), 4.83 (br s, 1H), 4.36–4.19 (m, 3H), 4.04–3.90 (m, 1H), 3.90–3.80 (m, 1H), 3.64–3.39 (m, 2H), 3.21 (br s, 1H), 3.14–2.89 (m, 4H), 2.86–2.69 (m,

4H), 2.38–2.11 (m, 2H), 1.82–1.73 (m, 1H), 1.66–1.46 (m, 6H), 1.43 (s, 9H), 1.39–1.26 (m, 1H), 0.95–0.85 (m, 6H). MS (Method B), *m/z* = 800 $[M + H]^+$.

Cbz-Orn(N-Boc)-Ser-Sta-NH(CH$_2$)$_2$Ph (64). General procedure B was followed using Boc-Ser-Sta-NH(CH$_2$)$_2$Ph (**43**) (46 mg, 0.114 mmol) and Cbz-Orn(N-Boc)-OH (42 mg, 0.114 mmol) to obtain Cbz-Orn(N-Boc)-Ser-Sta-NH(CH$_2$)$_2$Ph (**64**) as a solid (40 mg, 49%). ^{1}H-NMR (300 MHz; MeOD, rotamers): δ 7.56–7.17 (m, 10H), 5.12 (s, 2H), 4.38 (t, *J* = 5.0 Hz, 1H), 4.20–4.07 (m, 1H), 4.05–3.91 (m, 2H), 3.91–3.74 (m, 2H), 3.49–3.36 (m, 2H), 3.06 (t, *J* = 6.7 Hz, 2H), 2.89–2.74 (m, 2H), 2.38–2.21 (m, 2H), 1.93–1.76 (m, 1H), 1.76–1.51(m, 5H), 1.44 (s, 9H), 1.40–1.32 (m, 1H), 0.91 (d, *J* = 4.2 Hz, 3H), 0.93 (d, *J* = 4.2 Hz, 3H). MS (Method B), *m/z* = 714 $[M + H]^+$.

NH$_2$-β-hydroxy-Val-Sta-NH(CH$_2$)$_2$Ph (65). Fmoc-β-hydroxy-Val-Sta-NH(CH$_2$)$_2$Ph (**44**) (52 mg, 0.084 mmol) was dissolved in DCM/piperidine (1:1) (3 mL) and stirred for 1 h. The reaction mixture was then concentrated *in vacuo* and crude residue dissolved in EtOAc (30 mL) and washed with sat NaHCO$_3$ (20 mL), water (20 mL), brine (20 mL), dried with Na$_2$SO$_4$, filtered and concentrated *in vacuo*. The crude residue was then purified using a silica chromatography gradient eluting from 100% DCM to 15% MeOH/DCM to obtain NH$_2$-β-hydroxy-Val-Sta-NH(CH$_2$)$_2$Ph (**65**) as an oil (19 mg, 57%). ^{1}H-NMR (300 MHz; CDCl$_3$, rotamers): δ 7.65 (d, *J* = 9.7 Hz, 1H), 7.36–7.28 (m, 2H), 7.27–7.16 (m, 3H), 6.11–6.03 (m, 1H), 4.05–3.84 (m, 2H), 3.58–3.46 (m, 2H), 3.25 (s, 1H), 2.82 (t, *J* = 7.0 Hz, 2H), 2.30–2.22 (m, 2H), 1.72–1.50 (m, 5H), 1.43–1.34 (m, 1H), 1.28 (s, 3H), 1.17 (s, 3H), 0.95–0.88 (m, 6H). MS (Method B), *m/z* = 394 $[M + H]^+$.

Cbz-Orn(N-Boc)-β-hydroxy-Val-Sta-NH(CH$_2$)$_2$Ph (66). A mixture of the NH$_2$-β-hydroxy-Val-Sta-NH(CH$_2$)$_2$Ph (**65**) (19 mg, 0.048 mmol), Cbz-Orn(N-Boc)-OH (18 mg, 0.048 mmol), HBTU (24 mg, 0.063 mmol) and DIPEA (34 μL, 0.523 mmol) in DMF (1 mL) was allowed to stir for 18 h. The reaction mixture was quenched with 10% citric acid solution (10 mL) and the aqueous was

extracted with EtOAc (3 x 15 mL). The organic layers were combined, washed with saturated $NaHCO_3$ (1 x 15 mL), brine (1 x 15 mL), dried with Na_2SO_4, filtered and concentrated *in vacuo* to obtain the crude residue. The crude residue was purified using a silica chromatography gradient eluting from 100% DCM to 10% MeOH/DCM to obtain Cbz-Orn(N-Boc)-β-hydroxy-Val-Sta-$NH(CH_2)_2Ph$ (**66**) as an oil (17 mg, 47%). ^{1}H-NMR (300 MHz; $CDCl_3$, rotamers): δ 7.37–7.27 (m, 7H), 7.26–7.16 (m, 3H), 6.75–6.58 (m, 1H), 6.41–6.23 (m, 1H), 5.84–5.63 (m, 1H), 5.18–5.00 (m, 2H), 4.87–4.74 (m, 1H), 4.34–4.18 (m, 2H), 4.03–3.91 (m, 1H), 3.91–3.78 (m, 1H), 3.60–3.40 (m, 2H), 3.22–3.01 (m, 2H), 2.82 (t, *J* = 7.15 Hz, 2H), 2.38–2.26 (m, 1H), 2.24–2.14 (m, 1H), 1.87–1.62 (m, 5H), 1.61–1.48 (m, 4H), 1.43 (s, 9H), 1.38–1.32 (m, 1H), 1.30–1.15 (m, 6H), 0.94–0.77 (m, 6H). MS (Method B), *m/z* = 742 $[M + H]^+$.

Cbz-Orn(N-Boc)-Thr-Sta-$NH(CH_2)_2Ph$ (67). General procedure B was followed using Boc-Thr-Sta-$NH(CH_2)_2Ph$ (**45**) (57 mg, 0.120 mmol) and Cbz-Orn(N-Boc)-OH (41 mg, 0.113 mmol) to obtain Cbz-Orn(N-Boc)-Thr-Sta-$NH(CH_2)_2Ph$ (**67**) as a solid (46 mg, 53%). 1H-NMR (300 MHz, MeOD, rotamers): 7.41–7.19 (m, 10H), 5.13 (s, 2H), 4.32–4.13 (m, 3H), 4.05–3.93 (m, 2H), 3.46–3.37 (m, 2H), 3.11–3.01 (m, 2H), 2.81 (t, *J* = 7.5 Hz, 2H), 2.29 (d, *J* = 7.3 Hz, 2H), 1.92–1.78 (m, 1H), 1.74–1.51 (m, 5H), 1.44 (s, 9H), 1.41–1.29 (m, 2H), 1.22 (d, *J* = 6.6 Hz, 2H), 0.95–0.86 (m, 6H). MS (Method B), *m/z* = 728 $[M + H]^+$.

Cbz-Orn(N-Boc)-D,L-*threo*-β-phenyl-Ser-Sta-$NH(CH_2)_2Ph$ (68). General procedure B was followed using Boc-*threo*-β-phenyl-Ser-Sta-$NH(CH_2)_2Ph$ (**47**) (63 mg, 0.116 mmol) and Cbz-Orn(N-Boc)-OH (43 mg, 0.116 mmol) to obtain Cbz-Orn(N-Boc)-*threo*-β-phenyl-Ser-Sta-$NH(CH_2)_2Ph$ (**68**) as an oil (90 mg, 98%). ^{1}H-NMR (300 MHz; $CDCl_3$, rotamers): δ 7.47–7.28 (m, 12H), 7.27–7.13 (m, 3H), 7.03 (d, *J* = 9.0 Hz, 0.5H), 6.96-6.86 (m, 0.5H), 6.79 (br s, 0.5H), 6.49 (br s, 0.5H), 6.00–5.83 (m, 0.5H), 5.63–5.52 (m, 0.5H), 5.47 (br s, 0.5H), 5.32 (br s, 0.5H), 5.18–

4.88 (m, 2H), 4.82–4.10 (m, 4H), 4.06–3.82 (m, 3H), 3.55–3.34 (m, 2H), 3.07- 2.70 (m, 4H), 2.37–2.24 (m, 1H), 2.11–1.97 (m, 3H), 1.59–1.49 (m, 3H), 1.44 (m, 9H), 1.37–1.22 (m, 2H), 0.92–0.78 (m, 6H). MS (Method B), *m/z* = 790 $[M + H]^+$.

General Procedure C

Cbz-Arg(*N,N*-diBoc)-Val-Sta-NH$(CH_2)_2$Ph (69). A mixture of Cbz-Orn(*N*-Boc)-Val-Sta-NH$(CH_2)_2$Ph (**52**) (65 mg, 0.090 mmol) and 4M HCl in dioxane was allowed to stir for 1 h at 20 ºC. The reaction mixture was concentrated to dryness *in vacuo* to obtain the crude residue as a on oil. The oil was dissolved in DCM (1 mL) and Et_3N (6 µL, 0.043 mmol) was added. The solution was stirred vigorously for 5 min. *N,N'*-bis-Boc-1-guanylpyrazole (13 mg, 0.042 mmol) was added and the solution was allowed to stir for 18 h at 20 ºC. The reaction mixture was concentrated to dryness *in vacuo* to obtain a crude residue. The crude residue was subjected to a silica chromatography gradient eluting from 100% DCM to 10% MeOH/DCM to obtain Cbz-Arg(*N,N*-diBoc)-Val-Sta-NH$(CH_2)_2$Ph (**69**) as a solid (46 mg, 53%). ^{1}H-NMR (400 MHz; $CDCl_3$, rotamers): δ 8.63 (s, 1H), 7.61 (s, 1H), 7.41 (br s, 1H), 7.33-7.17 (m, 10H), 6.88 (br s, 2H), 6.34 (br s, 1H), 5.07-4.80 (m, 2H), 4.24 (q, *J* = 6.3 Hz, 1H), 4.17 (t, *J* = 7.1 Hz, 1H), 3.98-3.90 (m, 2H), 3.54-3.37 (m, 4H), 2.80 (t, *J* = 7.3 Hz, 2H), 2.37-2.14 (m, 3H), 1.88-1.84 (m, 1H), 1.73-1.53 (m, 6H), 1.48 (s, 9H), 1.46 (s, 9H), 1.37-1.30 (m, 1H), 0.93-0.84 (m, 12H). MS (Method A), *m/z* = 868 $[M + H]^+$.

Cbz-Arg(*N,N*-diBoc)-Ala-Sta-NH$(CH_2)_2$Ph (70). General procedure C was followed using Cbz-Orn(N-Boc)-Ala-Sta-NH$(CH_2)_2$Ph (**49**) (43 mg, 0.061 mmol) and *N,N'*-bis-Boc-1-guanylpyrazole (24 mg, 0.077 mmol) to obtain Cbz-Arg(*N,N*-diBoc)-Ala-Sta-NH$(CH_2)_2$Ph (**70**) (39 mg, 75%). ^{1}H-NMR (400 MHz, $CDCl_3$, rotamers): δ 11.43 (br s, 1H), 8.49 (br s, 1H), 7.35-7.14 (m, 10H), 6.73 (br s, 1H), 6.62 (d, *J* = 9.5 Hz, 1H), 6.51-6.49 (m, 1H), 5.08 (s, 2H), 4.39-4.32 (m, 1H), 4.20 (q, *J*

= 6.2 Hz, 1H), 3.99-3.93 (m, 1H), 3.89-3.88 (m, 1H), 3.54-3.35 (m, 4H), 2.82-2.75 (m, 2H), 2.75-2.60 (m, 2H), 2.33-2.16 (m, 2H), 1.87-1.83 (m, 1H), 1.77-1.41 (m, 23H), 1.41-1.17 (m, 6H), 0.88-0.86 (m, 6H). MS (Method B), *m/z* = 840 $[M + H]^+$.

Cbz-Arg(*N,N*-diBoc)-Abu-Sta-NH(CH$_2$)$_2$Ph (71). General procedure C was followed using Cbz-Orn(N-Boc)-Abu-Sta-NH(CH$_2$)$_2$Ph (**50**) (12 mg, 0.016 mmol) and *N,N'*-bis-Boc-1-guanylpyrazole (17 mg, 0.053 mmol) to obtain Cbz-Arg(*N,N*-diBoc)-Abu-Sta-NH(CH$_2$)$_2$Ph (**71**) (12 mg, 87%). ^{1}H-NMR (300 MHz, $CDCl_3$, rotamers): δ 11.46 (br s, 1H), 8.52 (br s, 1H), 7.39-7.19 (m, 10H), 6.99 (br s, 1H), 6.63-6.57 (m, 1H), 6.53-6.44 (m, 2H), 5.12 (s, 2H), 4.26-4.18 (m, 2H), 4.03-3.97 (m, 1H), 3.95-3.87 (m, 1H), 3.58-3.37 (m, 4H), 2.84 (t, *J* = 7.3 Hz, 2H), 2.38-2.19 (m, 3H), 1.92-1.84 (m, 2H), 1.79-1.54 (m, 4H), 1.49-1.44 (m, 18H), 1.41-1.06 (m, 3H), 0.99-0.79 (m, 9H). MS (Method B), *m/z* = 854 $[M + H]^+$.

Cbz-Arg(*N,N*-diBoc)-Nva-Sta-NH(CH$_2$)$_2$Ph (72). General procedure C was followed using Cbz-Orn(N-Boc)-Nva-Sta-NH(CH$_2$)$_2$Ph (**51**) (47 mg, 0.064 mmol) and *N,N'*-bis-Boc-1-guanylpyrazole (22 mg, 0.071 mmol) to obtain Cbz-Arg(*N,N*-diBoc)-Nva-Sta-NH(CH$_2$)$_2$Ph (**72**) as a solid (53 mg, 95%). ^{1}H-NMR (300 MHz; $CDCl_3$, rotamers): δ 11.46 (s, 1H), 8.46–8.29 (m, 1H), 7.60 (d, *J* = 2.2 Hz, 2H), 7.50–7.41 (m, 1H), 7.38–7.28 (m, 6H), 7.26–7.14 (m, 4H), 6.98–6.79 (m, 1H), 6.49 (d, *J* = 7.0 Hz, 1H), 6.33 (t, *J* = 2.0 Hz, 1H), 5.08 (s, 2H), 4.49–4.35 (m, 1H), 4.30–4.19 (m, 1H), 4.08–3.85 (m, 2H), 3.59–3.25 (m, 4H), 2.80 (t, *J* = 7.4 Hz, 2H), 2.40–2.21 (m, 2H), 1.86–1.52 (m, 7H), 1.47 (ad, *J* = 6.4 Hz, 18H), 1.40–1.23 (m, 3H), 0.97–0.78 (m, 9H). MS (Method B), *m/z* = 868 $[M+H]^+$.

Cbz-Arg(*N,N*-diBoc)-Leu-Sta-NH(CH$_2$)$_2$Ph (73). General procedure C was followed using Cbz-Orn(N-Boc)-Leu-Sta-NH(CH$_2$)$_2$Ph (**48**) (108 mg, 0.145 mmol) and *N,N'*-bis-Boc-1-guanylpyrazole (60 mg, 0.192 mmol) to obtain an impure mixture. The crude material was purified

by preparative LCMS to obtain Cbz-Arg(*N,N*-diBoc)-Leu-Sta-NH(CH_2)$_2$Ph (**73**) (32 mg, 24%). ^{1}H-NMR (300 MHz; $CDCl_3$, rotamers): δ 10.35 (br s, 1H), 9.02 (br s, 1H), 8.60 (br s, 1H), 8.29 (s, 1H), 8.11-7.98 (m, 1H), 7.81-7.58 (s, 1H), 7.40-7.12 (m, 10H), 7.00-6.36 (m, 2H), 6.34-6.17 (m, 1H), 5.17-5.02 (m, 2H), 4.47-4.18 (m, 2H), 4.05-3.82 (m, 2H), 3.63-3.28 (m, 4H) 3.30-3.09 (m, 1H), 2.88-2.76 (m, 2H), 2.73-2.45 (m, 2H), 2.41-2.20 (m, 2H), 2.05-1.92 (m, 2H), 1.84-1.40 (m, 18H) 1.42-1.02 (m, 3H), 1.02-0.76 (m, 12H). MS (Method A), *m/z* = 882, $[M + H]^+$.

Cbz-Arg(*N,N*-diBoc)-Ile-Sta-NH(CH_2)$_2$Ph (74). General procedure C was followed using Cbz-Orn(N-Boc)-Ile-Sta-NH(CH_2)$_2$Ph (**53**) (74 mg, 0.100 mmol) and *N,N'*-bis-Boc-1-guanylpyrazole (34 mg, 0.110 mmol). The crude material was purified by preparative LCMS to obtain Cbz-Arg(*N,N*-diBoc)-Ile-Sta-NH(CH_2)$_2$Ph (**74**) as a solid (44 mg, 49%). ^{1}H-NMR (300 MHz; $CDCl_3$, rotamers): δ 11.47 (s, 1H), 8.38 (t, *J* = 5.50 Hz, 1H), 7.37-7.27 (m, 6H), 7.26-7.14 (m, 4H), 6.87 (br s, 1H), 6.62 (d, *J* = 9.02 Hz, 1H), 6.40 (d, *J* = 6.6 Hz, 1H), 5.15–4.94 (m, 2H), 4.50 (br s, 1H), 4.25 (t, *J* = 7.6 Hz, 2H), 4.08–3.83 (m, 2H), 3.58–3.26 (m, 4H), 2.81 (t, *J* = 7.3 Hz, 2H), 2.38–2.18 (m, 2H), 1.96–1.72 (m, 3H), 1.71-1.52 (m, 6H), 1.47 (ad, *J* = 5.28 Hz, 18H), 1.41-1.21 (m, 1H), 1. 18-1.01 (m, 1H), 0.96-0.79 (m, 12H). MS (Method B), *m/z* = 882 $[M]^+$.

Cbz-Arg(*N,N*-diBoc)-tBuGly-Sta-NH(CH_2)$_2$Ph (75). General procedure C was followed using the crude mixture containing Cbz-Orn(N-Boc)-tBuGly-Sta-NH(CH_2)$_2$Ph (**54**) (39 mg, 0.052 mmol) and *N,N'*-bis-Boc-1-guanylpyrazole (26 mg, 0.083 mmol) to obtain Cbz-Arg(*N,N*-diBoc)-tBuGly-Sta-NH(CH_2)$_2$Ph (**75**) (42 mg, 91%). ^{1}H-NMR (300 MHz; $CDCl_3$, rotamers): δ 11.50-11.45 (m, 1H), 8.55 (s, 1H), 7.46-7.19 (m, 10H), 7.11-7.02 (m, 1H), 6.80-6.72 (m, 1H), 6.61-6.53 (m, 1H), 6.34-6.27 (m, 1H), 5.16-5.07 (m, 2H), 4.35-4.12 (m, 3H), 4.05-3.87 (m, 2H), 3.60-3.35 (m, 4H), 2.83 (t, *J* = 7.2 Hz, 2H), 2.42-2.32 (m, 1H), 2.28-2.19 (m, 1H), 1.92-1.79 (m, 1H), 1.79-

1.56 (m, 3H), 1.54-1.44 (m, 18H), 1.44-1.07 (m, 3H), 0.98 (s, 9H), 0.90-0.71 (m, 6H). MS (Method B), *m/z* = 883 $[M + H]^+$.

Cbz-Arg(*N,N*-diBoc)-EtNva-Sta-NH(CH$_2$)$_2$Ph (76). General procedure C was followed using Cbz-Orn(N-Boc)-EtNva-Sta-NH(CH$_2$)$_2$Ph (**55**) (63 mg, 0.082 mmol) and *N,N'*-bis-Boc-1-guanylpyrazole (34 mg, 0.109 mmol) to obtain Cbz-Arg(*N,N*-diBoc)-EtNva-Sta-NH(CH$_2$)$_2$Ph (**76**) (68 mg, 91%). ^{1}H-NMR (300 MHz, CDCl$_3$, rotamers): δ 11.49 (br s, 1H), 8.43-8.40 (m, 1H), 7.41-7.18 (m, 10H), 7.06 (br s, 1H), 6.80 (br s, 1H), 6.63-6.56 (m, 1H), 6.41-6.35 (m, 1H), 5.13-5.03 (m, 2H), 4.41 (t, *J* = 7.1 Hz, 1H), 4.33 (br s, 1H), 4.25-4.17 (m, 1H), 4.02-3.89 (m, 2H), 3.55-3.32 (m, 4H), 2.82 (t, *J* = 7.3 Hz, 2H), 2.37-2.23 (m, 2H), 1.91-1.14 (m, 30H), 0.96-0.80 (m, 12H). MS (Method B), *m/z* = 896 $[M + H]^+$.

Cbz-Arg(*N,N*-diBoc)-CyPenGly-Sta-NH(CH$_2$)$_2$Ph (77). General procedure C was followed using Cbz-Orn(N-Boc)-CyPenGly-Sta-NH(CH$_2$)$_2$Ph (**56**) (37 mg, 0.049 mmol) and *N,N'*-bis-Boc-1-guanylpyrazole (20 mg, 0.0655 mmol) to obtain Cbz-Arg(*N,N*-diBoc)-CyPenGly-Sta-NH(CH$_2$)$_2$Ph (**77**) (26 mg, 59%). ^{1}H-NMR (300 MHz, CDCl$_3$, rotamers): δ 11.48 (br s, 1H), 8.46-8.38 (m, 1H), 7.55-7.39 (m, 1H), 7.39-7.16 (m, 10H), 6.93 (br s, 1H), 6.69 (br s, 1H), 6.41-6.33 (m, 1H), 5.13-5.0 (m, 2H), 4.58 (s, 1H), 4.32-4.21 (m, 2H), 4.04-3.96 (m, 1H), 3.96-3.86 (m, 1H), 3.57-3.33 (m, 4H), 2.82 (t, *J* = 7.3 Hz, 2H), 2.38-2.20 (m, 2H), 1.89-1.78 (m, 1H), 1.78-1.41 (m, 28H), 1.41-1.15 (m, 5H), 0.89-0.82 (m, 6H). MS (Method B), *m/z* = 896 $[M + H]^+$.

Cbz-Arg(*N,N*-diBoc)-CyHexGly-Sta-NH(CH$_2$)$_2$Ph (78). General procedure C was followed using the crude mixture containing Cbz-Orn(N-Boc)-CyHexGly-Sta-NH(CH$_2$)$_2$Ph (**58**) (28 mg, 0.040 mmol) and *N,N'*-bis-Boc-1-guanylpyrazole (18 mg, 0.058 mmol) to obtain Cbz-Arg(*N,N*-diBoc)-CyHexGly-Sta-NH(CH$_2$)$_2$Ph (**78**) (36 mg, 98%). ^{1}H-NMR (300 MHz, CDCl$_3$): δ 11.47 (s, 1H), 8.56 (s, 1H), 7.42-7.17 (m, 10H), 6.85 (s, 1H), 6.70-6.56 (m, 1H), 6.40-6.33 (m, 1H), 5.14-

5.03 (m, 2H), 4.30-4.17 (m, 2H), 4.03-3.86 (m, 2H), 3.57-3.37 (m, 4H), 2.83 (t, *J* = 7.2 Hz, 2H), 2.41-2.22 (m, 2H), 1.92-1.54 (m, 12H), 1.53-1.46 (m, 18H), 1.44-0.95 (m, 8H), 0.89-0.82 (m, 6H). MS (Method B), *m/z* = 909 $[M + H]^+$.

Cbz-Arg(*N*,*N*-diBoc)-Phg-Sta-NH(CH$_2$)$_2$Ph (79). General procedure C was followed using Cbz-Orn(N-Boc)-Phg-Sta-NH(CH$_2$)$_2$Ph (**59**) (17 mg, 0.022 mmol) and *N,N'*-bis-Boc-1-guanylpyrazole (8 mg, 0.025 mmol) to obtain Cbz-Arg(*N,N*-diBoc)-Phg-Sta-NH(CH$_2$)$_2$Ph (**79**) as an oil (17 mg, 84%). ^{1}H-NMR (300 MHz; $CDCl_3$, rotamers): δ 11.47 (s, 1H), 8.40 (br s, 1H), 7.38–7.29 (m, 10H), 7.28–7.17 (m, 5H), 6.56–6.31 (m, 2H), 6.10 (br s, 1H), 5.36 (d, *J* = 6.2 Hz, 1H), 5.18–5.07 (m, 2H), 4.32–4.17 (m, 1H), 4.02–3.84 (m, 2H), 3.56–3.31 (m, 4H), 2.80 (t, *J* = 7.2 Hz, 2H), 2.11–1.55 (m, 10H), 1.51 (s, 9H), 1.49–1.44 (m, 1H), 1.40 (s, 9H), 0.96–0.86 (m, 6H). MS (Method B), *m/z* = 902 $[M]^+$.

Cbz-Arg(*N*,*N*-diBoc)-Phe-Sta-NH(CH$_2$)$_2$Ph (80). General procedure C was followed using Cbz-Orn(N-Boc)-Phe-Sta-NH(CH$_2$)$_2$Ph (**60**) (81 mg, 0.105 mmol) and *N,N'*-bis-Boc-1-guanylpyrazole (36 mg, 0.115 mmol) to obtain Cbz-Arg(*N,N*-diBoc)-Phe-Sta-NH(CH$_2$)$_2$Ph (**80**) as a solid (80 mg, 83%). ^{1}H-NMR (300 MHz; $CDCl_3$, rotamers): δ 11.43 (s, 1H), 8.36 (t, *J* = 5.7 Hz, 1H), 7.42–7.28 (m, 7H), 7.25–7.08 (m, 8H), 6.93 (d, *J* = 9.7 Hz, 1H), 6.44–6.27 (m, 2H), 6.14 (d, *J* = 6.4 Hz, 1H), 5.13–4.97 (m, 2H), 4.62 (q, *J* = 7.4 Hz, 1H), 4.19–4.07 (m, 1H), 3.96–3.84 (m, 2H), 3.84–3.77 (m, 1H), 3.61–3.37 (m, 2H), 3.32 (d, *J* = 5.7 Hz, 2H), 3.09 (dq, *J* = 7.2, 14.1 Hz, 2H), 2.83 (t, *J* = 7.3 Hz, 2H), 2.03–1.90 (m, 2H), 1.51–1.44 (m, 20H), 1.35–1.22 (m, 4H), 0.91–0.83 (m, 6H). MS (Method B), *m/z* = 916 $[M]^+$.

Cbz-Arg(*N*,*N*-diBoc)-β-phenyl-Phe-Sta-NH(CH$_2$)$_2$Ph (81). General procedure C was followed using Cbz-Orn(N-Boc)-β-phenyl-Phe-Sta-NH(CH$_2$)$_2$Ph (**61**) (61 mg, 0.072 mmol) and *N,N'*-bis-Boc-1-guanylpyrazole (25 mg, 0.079 mmol) to obtain Cbz-Arg(*N,N*-diBoc)-β-phenyl-Phe-Sta-

$NH(CH_2)_2Ph$ (**81**) as a solid (68 mg, 96%). ^{1}H-NMR (300 MHz; $CDCl_3$, rotamers): δ 11.41 (s, 1H), 8.28 (br s, 1H), 7.40–7.28 (m, 9H), 7.27–7.05 (m, 9H), 6.99–6.92 (m, 1H), 6.87 (d, *J* = 9.0 Hz, 1H), 6.38–6.17 (m, 2H), 5.80 (br s, 1H), 5.31–5.21 (m, 1H), 5.07 (d, *J* = 12.32 Hz, 1H), 4.91 (d, *J* = 12.8 Hz, 1H), 4.59 (d, *J* = 9.7 Hz, 1H), 4.21–4.10 (m, 1H), 3.83 (d, *J* = 6.1 Hz, 1H), 3.77-3.61 (m, 2H), 3.61–3.37 (m, 2H), 3.32–3.20 (m, 1H), 3.12 (d, *J* = 6.6 Hz, 1H), 2.88–2.78 (m, 2H), 1.66–1.55 (m, 4H), 1.55–1.46 (m, 18H), 1.46–1.30 (m, 4H), 1.30–1.21 (m, 2H), 0.90–0.67 (m, 6H). MS (Method B), *m/z* = 992 $[M]^+$.

Cbz-Arg(*N,N*-diBoc)-β-methyl-Phe-Sta-NH(CH$_2$)$_2$Ph (82). General procedure C was followed using Cbz-Orn(N-Boc)-β-methyl-Phe-Sta-$NH(CH_2)_2Ph$ (**62**) (62 mg, 0.079 mmol) and *N,N'*-bis-Boc-1-guanylpyrazole (27 mg, 0.087 mmol) to obtain Cbz-Arg(*N,N*-diBoc)-β-methyl-L-Phe-Sta-$NH(CH_2)_2Ph$ (**82**) as an oil (70 mg, 96%). ^{1}H-NMR (300 MHz; $CDCl_3$, rotamers): δ 11.47 (s, 1H), 8.42–8.26 (m, 1H), 7.61 (d, *J* = 1.8 Hz, 1H), 7.41–7.28 (m, 7H), 7.27–7.15 (m, 7H), 6.75–6.56 (m, 2H), 6.50 (d, *J* = 9.2 Hz, 1H), 6.35 (s, 1H), 6.07 (d, *J* = 5.5 Hz, 1H), 5.14 – 4.85 (m, 2H), 4.44 (t, *J* = 7.5 Hz, 1H), 4.03 – 3.83 (m, 3H), 3.59–3.40 (m, 3H), 3.34–3.22 (m, 2H), 2.87–2.79 (m, 2H), 2.35–2.15 (m, 2H), 1.73–1.52 (m, 3H), 1.50 (d, *J* = 7.3 Hz, 18H), 1.45–1.23 (m, 7H), 0.93–0.82 (m, 6H). MS (Method B), *m/z* = 930 $[M]^+$.

Cbz-Arg(*N,N*-diBoc)-2-indanylgly-Sta-NH(CH$_2$)$_2$Ph (83). General procedure C was followed using Cbz-Orn(N-Boc)-2-indanylgly-Sta-$NH(CH_2)_2Ph$ (**63**) (95 mg, 0.119 mmol) and *N,N'*-bis-Boc-1-guanylpyrazole (41 mg, 0.131 mmol) to obtain Cbz-Arg(*N,N*-diBoc)-2-indanylgly-Sta-$NH(CH_2)_2Ph$ (**83**) as a solid (91 mg, 81%). ^{1}H-NMR (300 MHz; $CDCl_3$, rotamers): δ 11.49 (s, 1H), 8.39 (br s, 1H), 7.61 (d, *J* = 1.54 Hz, 1H), 7.39–7.30 (m, 5H), 7.27–7.06 (m, 8H), 7.05–7.00 (m, 1H), 6.79 (d, *J* = 7.7 Hz, 1H), 6.70 (t, *J* = 5.3 Hz, 1H), 6.34 (s, 1H), 6.06 (d, *J* = 7.0 Hz, 1H), 5.08 (s, 2H), 4.53–4.38 (m, 1H), 4.20–4.09 (m, 1H), 4.07–4.00 (m, 1H), 3.99–3.89 (m, 1H), 3.81–

3.62 (m, 1H), 3.60–3.43 (m, 2H), 3.42–3.30 (m, 2H), 3.13–2.91 (m, 2H), 2.89–2.79 (m, 3H), 2.79–2.67 (m, 1H), 2.42–2.21 (m, 2H), 1.81–1.72 (m, 1H), 1.67–1.54 (m, 5H), 1.52–1.36 (m, 19H), 0.99–0.85. (m, 6H). MS (Method B), *m/z* = 942 $[M]^+$.

Cbz-Arg(*N,N*-diBoc)-Ser-Sta-NH(CH$_2$)$_2$Ph (84). General procedure C was followed using Cbz-Orn(N-Boc)-Ser-Sta-NH(CH$_2$)$_2$Ph (**64**) (40 mg, 0.056 mmol) and *N,N'*-bis-Boc-1-guanylpyrazole (19 mg, 0.061 mmol) to obtain Cbz-Arg(*N,N*-diBoc)-Ser-Sta-NH(CH$_2$)$_2$Ph (**84**) as an oil (20 mg, 48%). ^{1}H-NMR (300 MHz; $CDCl_3$, rotamers): δ 11.45 (s, 1H), 8.47–8.33 (m, 1H), 7.38–7.28 (m, 7H), 7.26–7.16 (m, 3H), 6.84–6.69 (m, 1H), 6.59–6.47 (m, 1H), 6.36 (d, *J* = 7.5 Hz, 1H), 5.18–5.04 (m, 2H), 4.49-4.38 (m, 1H), 4.26–4.15 (m, 1H), 4.08–3.85 (m, 3H), 3.79–3.69 (m, 1H), 3.56–3.29 (m, 4H), 2.81 (t, *J* = 7.4 Hz, 2H), 2.42–2.19 (m, 2H), 1.94–1.54 (m, 8H), 1.53–1.43 (m, 18H), 1.42–1.24 (m, 2H), 0.93–0.85 (m, 6H). MS (Method B), *m/z* = 856 $[M]^+$.

Cbz-Arg(*N,N*-diBoc)-β-hydroxy-Val-Sta-NH(CH$_2$)$_2$Ph (85). General procedure C was followed using Cbz-Orn(N-Boc)-β-hydroxy-Val-Sta-NH(CH$_2$)$_2$Ph (**66**) (16 mg, 0.022 mmol) and *N,N'*-bis-Boc-1-guanylpyrazole (7 mg, 0.023 mmol) to obtain Cbz-Arg(*N,N*-diBoc)-β-hydroxy-Val-Sta-NH(CH$_2$)$_2$Ph (**85**) as a solid (18 mg, 94%). ^{1}H-NMR (300 MHz; $CDCl_3$, rotamers): δ 11.48 (s, 1H), 8.44–8.31 (m, 1H), 7.36–7.27 (m, 7H), 7.27–7.17 (m, 3H), 7.16–7.02 (m, 1H), 6.77–6.62 (m, 1H), 6.50–6.32 (m, 1H), 6.32–6.14 (m, 1H), 5.19–5.02 (m, 2H), 4.46–3.77 (m, 6H), 3.60-3.29 (m, 4H), 2.82 (t, *J* = 7.0 Hz, 2H), 2.40-2.11 (m, 2H), 1.96-1.78 (m, 1H), 1.78-1.52 (m, 3H), 1.51-1.40 (m, 18H), 1.39-1.29 (m, 2H), 1.27 (s, 3H), 1.20–1.00 (m, 4H), 0.89-0.78 (m, 6H). MS (Method B), *m/z* = 884 $[M]^+$.

Cbz-Arg(*N,N*-diBoc)-Thr-Sta-NH(CH$_2$)$_2$Ph (86). General procedure C was followed using Cbz-Orn(N-Boc)-Thr-Sta-NH(CH$_2$)$_2$Ph (**67**) (46 mg, 0.063 mmol) and *N,N'*-bis-Boc-1-guanylpyrazole (22 mg, 0.070 mmol) to obtain Cbz-Arg(*N,N*-diBoc)-Thr-Sta-NH(CH$_2$)$_2$Ph (**86**) as an oil (50 mg,

91%). ^{1}H-NMR (300 MHz; $CDCl_3$, rotamers): δ 11.48 (s, 1H), 8.45–8.32 (m, 1H), 7.36–7.28 (m, 6H), 7.27–7.17 (m, 4H), 6.78 (d, *J* = 9.5 Hz, 1H), 6.57–6.43 (m, 1H), 6.38 (d, *J* = 6.4 Hz, 1H), 5.11 (s, 2H), 4.40–4.16 (m, 4H), 4.04–3.86 (m, 2H), 3.60–3.28 (m, 5H), 2.81 (t, *J* = 7.3 Hz, 2H), 2.41–2.19 (m, 2H), 2.03–1.82 (m, 3H), 1.80–1.52 (m, 5H), 1.52–1.41 (m, 18H), 1.39–1.31 (m, 1H), 1.16 (d, *J* = 5.9 Hz, 3H), 0.92–0.85 (m, 6 H). MS (Method B), *m/z* = 870 $[M]^+$.

Cbz-Arg(*N,N*-diBoc)-D,L-*threo*-β-phenyl-Ser-Sta-NH(CH$_2$)$_2$Ph (87). General procedure C was followed using Cbz-Orn(N-Boc)-*threo*-β-phenyl-Ser-Sta-NH(CH$_2$)$_2$Ph (**68**) (90 mg, 0.114 mmol) and *N,N'*-bis-Boc-1-guanylpyrazole (39 mg, 0.125 mmol) to obtain Cbz-Arg(*N,N*-diBoc)-*threo*-β-phenyl-Ser-Sta-NH(CH$_2$)$_2$Ph (**87**) as a solid (58 mg, 55%). ^{1}H-NMR (300 MHz; $CDCl_3$, rotamers): δ 11.48 (s, 1H), 8.34 (t, *J* = 5.8 Hz, 1H), 7.40–7.28 (m, 9H), 7.27–7.09 (m, 6H), 6.79 (d, *J* = 9.0 Hz, 1H), 6.37 (br s, 1H), 6.26 (d, *J* = 6.2 Hz, 1H), 5.50-5.35 (m, 1H), 5.19–5.02 (m, 2H), 4.78–4.58 (m, 1H), 4.15–4.02 (m, 2H), 4.02–3.87 (m, 2H), 3.87–3.74 (m, 1H), 3.56–3.39 (m, 2H), 3.38–3.17 (m, 2H), 2.87 -2.77 (m, 2H), 2.15–2.06 (m, 2H), 1.69–1.29 (m, 26H), 0.93–0.82 (m, 6H). MS (Method B), *m/z* = 932 $[M]^+$.

Cbz-Cav(N-Boc)-CyHexGly-Sta-NH(CH$_2$)$_2$Ph (88). General procedure A was followed using NH$_2$-CyHexGly-Sta-NH(CH$_2$)$_2$Ph (**57**) (82 mg, 0.198 mmol) and Cbz-Cav(N-Boc)-OH (58 mg, 0.141 mmol) to obtain Cbz-Cav(N-Boc)-CyHexGly-Sta-NH(CH$_2$)$_2$Ph (**88**) as an oil (75 mg, 65%). ^{1}H-NMR (300 MHz; $CDCl_3$, rotamers): δ 7.71–7.49 (m, 2H), 7.37–7.29 (m, 6H), 7.28-7.15 (m, 4H), 7.10–6.93 (m, 1H), 6.86–6.71 (m, 1H), 6.43–6.25 (m, 1H), 6.11 (br s, 2H), 5.16–5.02 (m, 2H), 4.62 (br s, 1H), 4.53–4.27 (m, 2H), 4.09–3.82 (m, 4H), 3.60–3.34 (m, 2H), 2.85–2.78 (m, 2H), 2.38–2.25 (m, 2H), 2.15 (br s, 1H), 2.04–1.90 (m, 1H), 1.83–1.54 (m, 8H), 1.53–1.46 (m, 9H), 1.42- 1.32 (m, 1H), 1.25–0.95 (m, 5H), 0.94–0.80 (m, 6H). MS (Method B), *m/z* = 810 $[M+H]^+$.

Cbz-Cav(N-Boc)-Phg-Sta-NH(CH_2)$_2$Ph (89). General procedure B was followed using Boc-Phg-Sta-NH(CH_2)$_2$Ph (**38**) (97 mg, 0.190 mmol) and Cbz-Cav(N-Boc)-OH (60 mg, 0.146 mmol). The crude material was purified by preparative LCMS to obtain Cbz-Cav(N-Boc)-Phg-Sta-NH(CH_2)$_2$Ph (**89**) as a solid (34 mg, 29%). ^{1}H-NMR (300 MHz; $CDCl_3$, rotamers): δ 8.38 (d, *J* = 5.3 Hz, 1H), 7.39–7.27 (m, 9H), 7.27–7.12 (m, 6H), 6.92 (d, *J* = 9.5 Hz, 1H), 6.46–6.24 (m, 2H), 6.20 (d, *J* = 6.6 Hz, 1H), 6.02–5.86 (m, 1H), 5.53 (d, *J* = 5.9 Hz, 1H), 5.07 (s, 2H), 4.56–4.44 (m, 1H), 4.08–3.79 (m, 4H), 3.48–3.31 (m, 2H), 2.74 (t, *J* = 7.0 Hz, 2H), 2.30–2.10 (m, 1H), 2.07–1.90 (m, 2H), 1.90–1.75 (m, 1H), 1.63–1.51 (m, 2H), 1.46 (s, 9H), 1.42–1.27 (m, 2H), 0.93–0.83 (m, 6H). MS (Method B), *m/z* = 804 $[M+H]^+$.

Cbz-Cav(N-Boc)-Ile-Sta-NH(CH_2)$_2$Ph (90). General procedure B was followed using Boc-Ile-Sta-NH(CH_2)$_2$Ph (**33**) (48 mg, 0.117 mmol) and Cbz-Cav(N-Boc)-OH (60 mg, 0.146 mmol) to obtain Cbz-Cav(N-Boc)-Ile-Sta-NH(CH_2)$_2$Ph (**90**) as a solid (32 mg, 35%). ^{1}H-NMR (300 MHz; $CDCl_3$, rotamers): δ 7.39 – 7.27 (m, 7H), 7.26 – 7.17 (m, 3H), 6.78 (d, *J* = 9.02 Hz, 1H), 6.71 – 6.56 (m, 1H), 6.30 (d, *J* = 6.6 Hz, 1H), 6.12 (br. s., 2H), 5.20 – 5.03 (m, 2H), 4.65 – 4.43 (m, 1H), 4.39 – 4.25 (m, 1H), 4.29 – 4.17 (m, 1H), 4.06 – 3.81 (m, 4H), 3.49 (dq, *J* = 6.1, 13.3 Hz, 2H), 2.87 – 2.77 (m, 2H), 2.41 – 2.08 (m, 4H), 2.05 – 1.83 (m, 2H), 1.63 – 1.52 (m, 2H), 1.49 - 1.31 (m, 10H), 1.16 – 1.00 (m, 1H), 0.98 – 0.77 (m, 12H). MS, *m/z* = 784 $[M+H]^+$.

Structural Biology Experimental

Protein expression and purification. *P. vivax* PMV (residues R35–R476), bearing an N-terminal gp67 signal peptide and a fusion tag comprising a FLAG tag, SUMO domain and tobacco etch virus (TEV) protease-cleavage site, was expressed in SF21 insect cells. Recombinant protein was purified initially from cell supernatant with anti-FLAG M2-agarose. Pooled fractions were

concentrated, and the N-terminal fusion tag was removed with TEV protease (1:25 (v/v), 5 h at room temperature, then overnight at 4°C). Gel-filtration chromatography (Superdex 75) in 20 mM HEPES, pH 7.2, 100 mM NaCl, and 0.2 mM DTT resulted in pure and stable protein that was concentrated for crystallization.

Structure determination. *P. vivax* PMV (11 mg/ml) was co-crystallized with **27** (8 molar excess) in 0.2 M ammonium sulfate, 25% (w/v) polyethylene glycol 3350, and 0.1 M bis-tris chloride, pH 5.5, at the CSIRO Collaborative Crystallization Centre. Crystals were frozen in well solution supplemented with 20% ethylene glycol. Data were collected at the Australian Synchrotron MX2 beamline at 100 K using the Australian Cancer Research Fund Eiger 16M detector. Data were processed with XDS [45, 46] Pointless [45] and Aimless [47] and the structure solved by molecular replacement with Phaser [48] using the PMV chain A protein component only from PDB 4ZL4 [37]. Further rounds of building and refinement with Coot [49] and Phenix [50], incorporating simulated annealing, yielded the final model. Restraints and co-ordinates for **27** were generated using the Grade server [51]. GlcNAc moieties were built using Coot into density for glycosylation (derived from insect cell expression).

Molecular modelling experimental. CLC Drug Discovery Workbench software (version 2.4.1) was used to minimize each P_2 analogue using the previously published *P. vivax* plasmepsin V crystal structure (PDB accession number 4ZL4) [37]. A 13Å radius binding site, centralized to binding region of WEHI-842 to plasmepsin V, was setup for minimalization of the input ligand. The water molecule present in the P_2 pocket of the X-ray crystal structure was retained for docking purposes. The input ligand was built into the program using the ligand designer and WEHI-842 as a template. To minimalize the binding conformation of the input ligand, CLC Drug Discovery Workbench uses a standard mode to determine the favorable binding poses, which detects various

flexible ligand conformations while holding protein as rigid structure during docking. The default number of iterations was set at 500. The ligand binding interactions of the resulting minimization were observed using the CLC Drug Discovery visualization tool and a score calculated. The docking data was then exported into PyMOL software for the visualization and output of the image seen in Figures S1-S4. The docking score used in the Drug Discovery Workbench is the $PLANTS_{PLP}$ [52].

Biology Experimental

Plasmepsin V fluorogenic PEXEL cleavage assays. Recombinant *P. vivax* plasmepsin V and PEXEL cleavage assays were performed as described previously [37]. Briefly, *P. vivax* plasmepsin V was recombinantly expressed and purified from High Five insect cells using anti-FLAG M2-agarose followed by Gel-filtration chromatography (Superdex 75). Reactions included a fluorescent peptide of nine amino acids containing the PEXEL (RTLAQ) sequence from KAHRP [29]. The KAHRP PEXEL peptide substrate DABCYL-RNKRTLAQKQ-E-EDANS was obtained commercially and used at a final assay concentration of 12 μM (the Km of the substrate). The end-point for all assays was set within the linear range of activity (approximately 1 h). Tween-20 was used at 0.005% final assay concentration. The final assay buffer concentration was as follows: 25 mM Tris HCl and 25 mM MES, pH 6.4. The final assay volume was 20 μL which consisted of 2.5 ng per well of recombinant *P. vivax* plasmepsin V. A ten-point 1-in-3 serial dilution of compounds was generated using DMSO as a vehicle (final assay concentration of 1%). Assay reactions were incubated for 120 min at 37°C and read using a fluorescence plate reader (ex, 340 nm; em, 495 nm). IC_{50} values were determined using a nonlinear regression four-parameter fit analysis, using GraphPad Prism software, where two of the parameters were constrained to 0 and 100%.

Parasite PEXEL processing assay, immunoblot, and densitometry. *P. falciparum* 3D7 were cultured in human O^+ erythrocytes at 4% hematocrit in RPMI 1640 medium supplemented with 25 mM HEPES, pH 7.4, 0.2% sodium bicarbonate, and 0.5% Albumax II (Invitrogen) in culture gas (5% CO_2, 5% O_2, 90% N) at 37ºC. *P. falciparum* 3D7 expressing PfEMP3-GFP were as generated previously [29] and treated with compounds as described previously [35]. Briefly, 24−34 h old trophozoites were purified from uninfected erythrocytes by passing the culture through a Vario Macs magnet column (Miltenyi Biotech) and cells treated with inhibitor for 3 h at 37°C in culture gas. Parasites were treated with 0.1% saponin to liberate contaminating hemoglobin and pellets solubilized in 4× Laemmli sample buffer before protein separation via SDS-PAGE. Proteins were transferred to nitrocellulose, blocked in 10% skim milk/PBS-T (0.05%) and probed with mouse anti-GFP (Roche; 1:1000 in 1% skim milk/PBS-T) or rabbit anti-HSP70 (Roche; 1:2000 in 1% skim milk/PBS-T) antibodies followed by horseradish peroxidase-conjugated secondary antibodies (goat α-mouse; Silenius; 1:1000 in 1% skim milk/PBS-T) and visualized using enhanced chemiluminescence (GE Amersham). Blots were exposed within the linear range using film or the ChemiDoc™ Touch system (Bio-Rad), imaged or scanned and then quantified in Image Lab (Bio-Rad).

Parasite viability assay. Parasite viability assays were performed as described by Gamo *et al* [53]. Briefly, *P. falciparum* 3D7 parasites were cultured according to the procedure described by Jensen *et al.* [54] in RPMI-HEPES media supplemented with L-glutamine and Albumax II. Early ring-stage *P. falciparum* 3D7 parasites were obtained by sorbitol synchronization and incubated with compounds solubilized in DMSO (not greater than 0.02% final to limit toxicity) in ten-point titrations. Parasitemia was determined at 72 h using a lactate dehydrogenase (LDH) readout as a percentage relative to the DMSO vehicle control. Values were plotted using a 4-parameter log

dose, non-linear regression analysis, with sigmoidal dose response (variable slope) curve fit in GraphPad Prism (ver 6.05) to generate drug curves and EC_{50} values.

HepG2 cell growth inhibition assay. The cell growth inhibition assays were performed as described by Gilson *et al* [44]. Briefly, HepG2 cells were cultured in Dulbecco's Modified Eagles Medium (DME) supplemented with 10% fetal calf serum (FCS) in a humidified incubator at 37°C and 5% CO_2. Cells (1×10^4) were seeded in 384 well assay plates and incubated with compounds (10-point titration) for 48 hr. Cytotoxicity was determined using Cell Titer Glo. Percent viability was normalized to DMSO controls (100% viability) and 10 μM bortezomib (0% viability). The EC_{50} was calculated using a four-parameter logistic nonlinear regression model.

ASSOCIATED CONTENT

Supporting Information. Chemistry and biology experimental; compound dose response data; molecular modeling and X-ray data. The Supporting Information is available free of charge on the ACS Publications website.

Accession Code. PDB codes for the X-ray crystal structures described in this study have been deposited in the PDB under the accession code 6C4G.

ACKNOWLEDGMENTS

This work was funded by the National Health and Medical Research Council of Australia (Development Grant 1113712 to B.E.S. Project Grant 1092789 and Program Grant 1092789 to A.F.C.), a CASS Foundation Science and Medicine Grant SM/15/6430 to J.A.B., the Australian

Cancer Research Foundation, the Victorian State Government Operational Infrastructure Support and Australian Government NHMRC IRIISS. A.F.C. is a Howard Hughes International Scholar. P.E.C and J.A.B are NHMRC Research Fellows (1079700 and 1123727, respectively). X-ray diffraction data was collected on the MX2 beamline at the Australian Synchrotron and made use of the ACRF Detector.

ABBREVIATIONS

Abu – aminobutyric acid; Cav – canavanine; CyHexGly – cyclohexylglycine; CyPenGly – cyclopentylglycine; EtNva – beta-ethyl-norvaline; GFP – green fluorescent protein; HBTU – O-(benzotriazol-1-yl)-*N,N,N′,N′*-tetramethyluronium hexafluorophosphate; β-hydroxy-Val – β-hydroxy-valine; 2-indanylGly – 2-indanyl glycine; KAHRP – knob associated histidine rich protein; LDH – lactate dehydrogenase; β-methyl-Phe – (2*S*,3*S*) *erythro*-L-β-methyl-phenylalanine; Nva – norvaline; Orn – ornithine; PfEMP3 – *P. falciparum* erythrocyte membrane protein 3; PMV – plasmepsin V; PEXEL – *Plasmodium* export element; Pf – *Plasmodium falciparum*; β-phenyl-Phe – 3,3-diphenyl alanine; *threo*-β-phenyl-Ser – D,L-*threo*-β-phenyl serine; Pv – *Plasmodium vivax*; Sta – (3*S*,4*S*)-4-amino-3-hydroxy-6-methylheptanoic acid; tBuGly – *tert*-butyl glycine; TFA – trifluoroacetic acid.

REFERENCES

[1] World Malaria Report 2016. World Health Organisation, Geneva. http://www.who.int/malaria/publications/world-malaria-report-2016/report/en/23 (accessed Dec. 23, 2016).

[2] I.H. Cheeseman, B.A. Miller, S. Nair, S. Nkhoma, A. Tan, J.C. Tan, S. Al Saai, A.P. Phyo, C.L. Moo, K.M. Lwin, R. McGready, E. Ashley, M. Imwong, K. Stepniewska, P. Yi, A.M.

Dondorp, M. Mayxay, P.N. Newton, N.J. White, F. Nosten, M.T. Ferdig, T.J. Anderson, A major genome region underlying artemisinin resistance in malaria, Science (New York, N.Y.), 336 (2012) 79-82.

[3] S. Takala-Harrison, T.G. Clark, C.G. Jacob, M.P. Cummings, O. Miotto, A.M. Dondorp, M.M. Fukuda, F. Nosten, H. Noedl, M. Imwong, D. Bethell, Y. Se, C. Lon, S.D. Tyner, D.L. Saunders, D. Socheat, F. Ariey, A.P. Phyo, P. Starzengruber, H.P. Fuehrer, P. Swoboda, K. Stepniewska, J. Flegg, C. Arze, G.C. Cerqueira, J.C. Silva, S.M. Ricklefs, S.F. Porcella, R.M. Stephens, M. Adams, L.J. Kenefic, S. Campino, S. Auburn, B. MacInnis, D.P. Kwiatkowski, X.Z. Su, N.J. White, P. Ringwald, C.V. Plowe, Genetic loci associated with delayed clearance of *Plasmodium falciparum* following artemisinin treatment in Southeast Asia, Proc. Natl. Acad. Sci. U.S.A., 110 (2013) 240-245.

[4] R. Banerjee, J. Liu, W. Beatty, L. Pelosof, M. Klemba, D.E. Goldberg, Four plasmepsins are active in the *Plasmodium falciparum* food vacuole, including a protease with an active-site histidine, Proceedings of the National Academy of Sciences of the United States of America, 99 (2002) 990-995.

[5] J. Liu, I.Y. Gluzman, M.E. Drew, D.E. Goldberg, The role of *Plasmodium falciparum* food vacuole plasmepsins, The Journal of biological chemistry, 280 (2005) 1432-1437.

[6] J.A. Bonilla, T.D. Bonilla, C.A. Yowell, H. Fujioka, J.B. Dame, Critical roles for the digestive vacuole plasmepsins of *Plasmodium falciparum* in vacuolar function, Mol. Microbiol., 65 (2007) 64-75.

[7] J.A. Bonilla, P.A. Moura, T.D. Bonilla, C.A. Yowell, D.A. Fidock, J.B. Dame, Effects on growth, hemoglobin metabolism and paralogous gene expression resulting from disruption of genes encoding the digestive vacuole plasmepsins of *Plasmodium falciparum*, Int. J. Parasitol., 37 (2007) 317-327.

[8] J. Liu, E.S. Istvan, I.Y. Gluzman, J. Gross, D.E. Goldberg, *Plasmodium falciparum* ensures its amino acid supply with multiple acquisition pathways and redundant proteolytic enzyme systems, Proc. Natl. Acad. Sci. U.S.A., 103 (2006) 8840-8845.

[9] A.L. Omara-Opyene, P.A. Moura, C.R. Sulsona, J.A. Bonilla, C.A. Yowell, H. Fujioka, D.A. Fidock, J.B. Dame, Genetic disruption of the *Plasmodium falciparum* digestive vacuole plasmepsins demonstrates their functional redundancy, J. Biol. Chem., 279 (2004) 54088-54096.

[10] A. Ecker, E.S. Bushell, R. Tewari, R.E. Sinden, Reverse genetics screen identifies six proteins important for malaria development in the mosquito, Molecular microbiology, 70 (2008) 209-220.

[11] B.S. Mastan, S.K. Narwal, S. Dey, K.A. Kumar, S. Mishra, *Plasmodium berghei* plasmepsin VIII is essential for sporozoite gliding motility, International journal for parasitology, 47 (2017) 239-245.

[12] B.S. Mastan, A. Kumari, D. Gupta, S. Mishra, K.A. Kumar, Gene disruption reveals a dispensable role for plasmepsin VII in the *Plasmodium berghei* life cycle, Mol. Biochem. Parasitol., 195 (2014) 10-13.

[13] A.S. Nasamu, S. Glushakova, I. Russo, B. Vaupel, A. Oksman, A.S. Kim, D.H. Fremont, N. Tolia, J.R. Beck, M.J. Meyers, J.C. Niles, J. Zimmerberg, D.E. Goldberg, Plasmepsins IX and X

are essential and druggable mediators of malaria parasite egress and invasion, Science (New York, N.Y.), 358 (2017) 518-522.

[14] P. Pino, R. Caldelari, B. Mukherjee, J. Vahokoski, N. Klages, B. Maco, C.R. Collins, M.J. Blackman, I. Kursula, V. Heussler, M. Brochet, D. Soldati-Favre, A multistage antimalarial targets the plasmepsins IX and X essential for invasion and egress, Science (New York, N.Y.), 358 (2017) 522-528.

[15] V. Aureggi, V. Ehmke, J. Wieland, W.B. Schweizer, B. Bernet, D. Bur, S. Meyer, M. Rottmann, C. Freymond, R. Brun, B. Breit, F. Diederich, Potent inhibitors of malarial aspartic proteases, the plasmepsins, by hydroformylation of substituted 7-azanorbornenes, Chemistry (Weinheim an der Bergstrasse, Germany), 19 (2013) 155-164.

[16] C. Boss, O. Corminboeuf, C. Grisostomi, S. Meyer, A.F. Jones, L. Prade, C. Binkert, W. Fischli, T. Weller, D. Bur, Achiral, cheap, and potent inhibitors of Plasmepsins I, II, and IV, ChemMedChem, 1 (2006) 1341-1345.

[17] C. Boss, S. Richard-Bildstein, T. Weller, W. Fischli, S. Meyer, C. Binkert, Inhibitors of the *Plasmodium falciparum* parasite aspartic protease plasmepsin II as potential antimalarial agents, Current medicinal chemistry, 10 (2003) 883-907.

[18] K. Jaudzems, K. Tars, G. Maurops, N. Ivdra, M. Otikovs, J. Leitans, I. Kanepe-Lapsa, I. Domraceva, I. Mutule, P. Trapencieris, M.J. Blackman, A. Jirgensons, Plasmepsin inhibitory activity and structure-guided optimization of a potent hydroxyethylamine-based antimalarial hit, ACS medicinal chemistry letters, 5 (2014) 373-377.

[19] T. Miura, K. Hidaka, T. Uemura, K. Kashimoto, Y. Hori, Y. Kawasaki, A.J. Ruben, E. Freire, T. Kimura, Y. Kiso, Improvement of both plasmepsin inhibitory activity and antimalarial activity by 2-aminoethylamino substitution, Bioorganic & medicinal chemistry letters, 20 (2010) 4836-4839.

[20] D. Noteberg, W. Schaal, E. Hamelink, L. Vrang, M. Larhed, High-speed optimization of inhibitors of the malarial proteases plasmepsin I and II, J. Comb. Chem., 5 (2003) 456-464.

[21] K.M. Orrling, M.R. Marzahn, H. Gutierrez-de-Teran, J. Aqvist, B.M. Dunn, M. Larhed, alpha-Substituted norstatines as the transition-state mimic in inhibitors of multiple digestive vacuole malaria aspartic proteases, Bioorg. Med. Chem., 17 (2009) 5933-5949.

[22] D. Rasina, M. Otikovs, J. Leitans, R. Recacha, O.V. Borysov, I. Kanepe-Lapsa, I. Domraceva, T. Pantelejevs, K. Tars, M.J. Blackman, K. Jaudzems, A. Jirgensons, Fragment-based discovery of 2-aminoquinazolin-4(3H)-ones as novel class nonpeptidomimetic inhibitors of the plasmepsins I, II, and IV, J. Med. Chem., 59 (2016) 374-387.

[23] J.A. Boddey, T.G. Carvalho, A.N. Hodder, T.J. Sargeant, B.E. Sleebs, D. Marapana, S. Lopaticki, T. Nebl, A.F. Cowman, Role of plasmepsin V in export of diverse protein families from the *Plasmodium falciparum* exportome, Traffic, 14 (2013) 532-550.

[24] A. Heiber, F. Kruse, C. Pick, C. Gruring, S. Flemming, A. Oberli, H. Schoeler, S. Retzlaff, P. Mesen-Ramirez, J.A. Hiss, M. Kadekoppala, L. Hecht, A.A. Holder, T.W. Gilberger, T. Spielmann, Identification of new PNEPs indicates a substantial non-PEXEL exportome and underpins common features in *Plasmodium falciparum* protein export, PLoS Pathog., 9 (2013) e1003546.

[25] T.J. Sargeant, M. Marti, E. Caler, J.M. Carlton, K. Simpson, T.P. Speed, A.F. Cowman, Lineage-specific expansion of proteins exported to erythrocytes in malaria parasites, Genome Biol., 7 (2006) R12.

[26] A.G. Maier, M. Rug, M.T. O'Neill, M. Brown, S. Chakravorty, T. Szestak, J. Chesson, Y. Wu, K. Hughes, R.L. Coppel, C. Newbold, J.G. Beeson, A. Craig, B.S. Crabb, A.F. Cowman, Exported proteins required for virulence and rigidity of *Plasmodium falciparum*-infected human erythrocytes, Cell, 134 (2008) 48-61.

[27] M. Marti, R.T. Good, M. Rug, E. Knuepfer, A.F. Cowman, Targeting malaria virulence and remodeling proteins to the host erythrocyte, Science (New York, N.Y.), 306 (2004) 1930-1933.

[28] N.L. Hiller, S. Bhattacharjee, C. van Ooij, K. Liolios, T. Harrison, C. Lopez-Estrano, K. Haldar, A host-targeting signal in virulence proteins reveals a secretome in malarial infection, Science (New York, N.Y.), 306 (2004) 1934-1937.

[29] J.A. Boddey, A.N. Hodder, S. Gunther, P.R. Gilson, H. Patsiouras, E.A. Kapp, J.A. Pearce, T.F. de Koning-Ward, R.J. Simpson, B.S. Crabb, A.F. Cowman, An aspartyl protease directs malaria effector proteins to the host cell, Nature, 463 (2010) 627-631.

[30] I. Russo, S. Babbitt, V. Muralidharan, T. Butler, A. Oksman, D.E. Goldberg, Plasmepsin V licenses *Plasmodium* proteins for export into the host erythrocyte, Nature, 463 (2010) 632-636.

[31] J.A. Boddey, M.T. O'Neill, S. Lopaticki, T.G. Carvalho, A.N. Hodder, T. Nebl, S. Wawra, P. van West, Z. Ebrahimzadeh, D. Richard, S. Flemming, T. Spielmann, J. Przyborski, J.J. Babon, A.F. Cowman, Export of malaria proteins requires co-translational processing of the

PEXEL motif independent of phosphatidylinositol-3-phosphate binding, Nat. Commun., 7 (2016) 10470.

[32] H.H. Chang, A.M. Falick, P.M. Carlton, J.W. Sedat, J.L. DeRisi, M.A. Marletta, N-terminal processing of proteins exported by malaria parasites, Mol. Biochem. Parasitol., 160 (2008) 107-115.

[33] M. Rug, M. Cyrklaff, A. Mikkonen, L. Lemgruber, S. Kuelzer, C.P. Sanchez, J. Thompson, E. Hanssen, M. O'Neill, C. Langer, M. Lanzer, F. Frischknecht, A.G. Maier, A.F. Cowman, Export of virulence proteins by malaria-infected erythrocytes involves remodeling of host actin cytoskeleton, Blood, 124 (2014) 3459-3468.

[34] B.E. Sleebs, M. Gazdik, M.T. O'Neill, P. Rajasekaran, S. Lopaticki, K. Lackovic, K. Lowes, B.J. Smith, A.F. Cowman, J.A. Boddey, Transition state mimetics of the *Plasmodium* export element are potent inhibitors of plasmepsin V from *P. falciparum* and *P. vivax*, J. Med. Chem., 57 (2014) 7644-7662.

[35] B.E. Sleebs, S. Lopaticki, D.S. Marapana, M.T. O'Neill, P. Rajasekaran, M. Gazdik, S. Gunther, L.W. Whitehead, K.N. Lowes, L. Barfod, L. Hviid, P.J. Shaw, A.N. Hodder, B.J. Smith, A.F. Cowman, J.A. Boddey, Inhibition of plasmepsin V activity demonstrates its essential role in protein export, PfEMP1 display, and survival of Malaria parasites, PLoS Biol., 12 (2014) e1001897.

[36] M. Gazdik, K.E. Jarman, M.T. O'Neill, A.N. Hodder, K.N. Lowes, H. Jousset Sabroux, A.F. Cowman, J.A. Boddey, B.E. Sleebs, Exploration of the P3 region of PEXEL peptidomimetics

leads to a potent inhibitor of the *Plasmodium* protease, plasmepsin V, Bioorg. Med. Chem., 24 (2016) 1993-2010.

[37] A.N. Hodder, B.E. Sleebs, P.E. Czabotar, M. Gazdik, Y. Xu, M.T. O'Neill, S. Lopaticki, T. Nebl, T. Triglia, B.J. Smith, K. Lowes, J.A. Boddey, A.F. Cowman, Structural basis for plasmepsin V inhibition that blocks export of malaria proteins to human erythrocytes, Nat. Struct. Mol. Biol., 22 (2015) 590-596.

[38] L. Gambini, L. Rizzi, A. Pedretti, O. Taglialatela-Scafati, M. Carucci, A. Pancotti, C. Galli, M. Read, E. Giurisato, S. Romeo, I. Russo, Picomolar inhibition of plasmepsin V, an essential Malaria protease, achieved exploiting the prime region, PLoS One, 10 (2015) e0142509.

[39] M. Gazdik, M.T. O'Neill, S. Lopaticki, K.N. Lowes, B.J. Smith, A.F. Cowman, J.A. Boddey, B.E. Sleebs, The effect of N-methylation on transition state mimetic inhibitors of the *Plasmodium* protease, plasmepsin V, MedChemComm, 6 (2015) 437-443.

[40] S.B.H. Kent, A.R. Mitchell, M. Engelhard, R.B. Merrifield, Mechanisms and prevention of trifluoroacetylation in solid-phase peptide synthesis, Proc. Natl. Acad. Sci. U.S.A., 76 (1979) 2180-2184.

[41] M.B.-U. Surfraz, R. King, S.J. Mather, S.C.G. Biagini, P.J. Blower, Trifluoroacetyl-HYNIC peptides: Synthesis and 99mTc radiolabeling, J. Med. Chem., 50 (2007) 1418-1422.

[42] B.S. Crabb, B.M. Cooke, J.C. Reeder, R.F. Waller, S.R. Caruana, K.M. Davern, M.E. Wickham, G.V. Brown, R.L. Coppel, A.F. Cowman, Targeted gene disruption shows that knobs enable malaria-infected red cells to cytoadhere under physiological shear stress, Cell, 89 (1997) 287-296.

[43] Calculator Plugins were used for structure property prediction and calculation. MarvinSketch 6.0.6., ChemAxon (http://www.chemaxon.com).

[44] P.R. Gilson, C. Tan, K.E. Jarman, K.N. Lowes, J.M. Curtis, W. Nguyen, A.E. Di Rago, H.E. Bullen, B. Prinz, S. Duffy, J.B. Baell, C.A. Hutton, H. Jousset Subroux, B.S. Crabb, V.M. Avery, A.F. Cowman, B.E. Sleebs, Optimization of 2-anilino 4-amino substituted qinazolines into potent antimalarial agents with oral *in vivo* activity, J. Med. Chem., 60 (2017) 1171-1188.

[45] P.R. Evans, An introduction to data reduction: space-group determination, scaling and intensity statistics, Acta Crystallogr. D Biol. Crystallogr., 67 (2011) 282-292.

[46] W. Kabsch, XDS, Acta Crystallogr. D Biol. Crystallogr., 66 (2010) 125-132.

[47] P.R. Evans, G.N. Murshudov, How good are my data and what is the resolution?, Acta Crystallogr. D Biol. Crystallogr., 69 (2013) 1204-1214.

[48] A.J. McCoy, R.W. Grosse-Kunstleve, P.D. Adams, M.D. Winn, L.C. Storoni, R.J. Read, Phaser crystallographic software, J. Appl. Crystallogr., 40 (2007) 658-674.

[49] P. Emsley, K. Cowtan, Coot: model-building tools for molecular graphics, Acta crystallographica. Section D, Biological crystallography, 60 (2004) 2126-2132.

[50] P.D. Adams, P.V. Afonine, G. Bunkoczi, V.B. Chen, I.W. Davis, N. Echols, J.J. Headd, L.W. Hung, G.J. Kapral, R.W. Grosse-Kunstleve, A.J. McCoy, N.W. Moriarty, R. Oeffner, R.J. Read, D.C. Richardson, J.S. Richardson, T.C. Terwilliger, P.H. Zwart, PHENIX: a comprehensive Python-based system for macromolecular structure solution, Acta Crystallogr. D Biol. Crystallogr., 66 (2010) 213-221.

[51] O.S. Smart, T.O. Womack, A. Sharff, C. Flensburg, P. Keller, W. Paciorek, C. Vonrhein, G. Bricogne, Grade v.1.2.9., Cambridge: Global Phasing Ltd., (2014).

[52] O. Korb, T. Stutzle, T.E. Exner, Empirical scoring functions for advanced protein-ligand docking with PLANTS, J. Chem. Inf. Model., 49 (2009) 84-96.

[53] F.J. Gamo, L.M. Sanz, J. Vidal, C. de Cozar, E. Alvarez, J.L. Lavandera, D.E. Vanderwall, D.V. Green, V. Kumar, S. Hasan, J.R. Brown, C.E. Peishoff, L.R. Cardon, J.F. Garcia-Bustos, Thousands of chemical starting points for antimalarial lead identification, Nature, 465 (2010) 305-310.

[54] W. Trager, J.B. Jensen, Human malaria parasites in continuous culture, Science, 193 (1976) 673-675.

GRAPHICAL ABSTRACT